



Spring 1994

# Downstream Fining in a Mountain Stream Channel Affected by Debris Flow

Craig Emerson Cooper  
*Western Washington University*

Follow this and additional works at: <https://cedar.wwu.edu/wwuet>



Part of the [Geology Commons](#)

---

## Recommended Citation

Cooper, Craig Emerson, "Downstream Fining in a Mountain Stream Channel Affected by Debris Flow" (1994). *WWU Graduate School Collection*. 821.

<https://cedar.wwu.edu/wwuet/821>

This Masters Thesis is brought to you for free and open access by the WWU Graduate and Undergraduate Scholarship at Western CEDAR. It has been accepted for inclusion in WWU Graduate School Collection by an authorized administrator of Western CEDAR. For more information, please contact [westerncedar@wwu.edu](mailto:westerncedar@wwu.edu).

DOWNSTREAM FINING IN A MOUNTAIN STREAM CHANNEL  
AFFECTED BY DEBRIS FLOW

by

Craig Emerson Cooper

Accepted in Partial Completion  
of the Requirements for the Degree  
Master of Science

---

Dean of Graduate School

Advisory Committee

Chair

## MASTER'S THESIS

In presenting this thesis in partial fulfillment of the requirements for a master's degree at Western Washington University, I agree that the Library shall make its copies freely available for inspection. I further agree that extensive copying of this thesis is allowable only for scholarly purposes. It is understood, however, that any copying or publication of this thesis for commercial purposes, or for financial gain, shall not be allowed without my written permission.

Signature

Date MAY 20, 1994

## MASTER'S THESIS

In presenting this thesis in partial fulfillment of the requirements for a master's degree at Western Washington University, I grant to Western Washington University the non-exclusive royalty-free right to archive, reproduce, distribute, and display the thesis in any and all forms, including electronic format, via any digital library mechanisms maintained by WWU.

I represent and warrant this is my original work and does not infringe or violate any rights of others. I warrant that I have obtained written permissions from the owner of any third party copyrighted material included in these files.

I acknowledge that I retain ownership rights to the copyright of this work, including but not limited to the right to use all or part of this work in future works, such as articles or books.

Library users are granted permission for individual, research and non-commercial reproduction of this work for educational purposes only. Any further digital posting of this document requires specific permission from the author.

Any copying or publication of this thesis for commercial purposes, or for financial gain, is not allowed without my written permission.

Name: CRAIG ERNESTON COOPER

Signature: 

Date: MAY 26, 2018

DOWNSTREAM FINING IN A MOUNTAIN STREAM CHANNEL  
AFFECTED BY DEBRIS FLOW

A Thesis  
Presented to  
The Faculty of  
Western Washington University

In Partial Fulfillment  
of the Requirements for the Degree  
Master of Science

by  
Craig Emerson Cooper  
May, 1994



## **ABSTRACT**

Grain size of particles tend to become smaller in the downstream direction. Abrasion and selective transport are two sets of processes commonly accepted as explanations for observed trends in fining of sediment. Most recent studies have emphasized the effectiveness of selective transport in producing downstream fining in streams with abundant sediment supply. The contribution of abrasion to particle fining of the coarsest class of particles was investigated in Finney Creek, a high gradient mountain stream in northwest Washington that has a high incidence of sedimentation from debris slides and debris flows. Two dominant rock types comprise the coarsest bed material in the studied reach; foliated particles, which are derived from the local bedrock, and non-foliated particles, which are derived from glacial valley fill. Four distinct downstream trends of particle fining are spatially associated with sources of recent deposits of coarse clasts in the channel. While particle sizes of both rock types diminish rapidly from the debris source, overall fining trends are influenced most by the fining trend evident in the foliated class of particles. The primary fining mechanisms are different for the two rock types, and are related most strongly to the inherent durability of each rock type. Selective transport is probably most important for non-foliated particles, and active but overwhelmed by abrasion for foliated particles. Field observations and experimental abrasion studies indicate that abrasion is the dominant set of processes responsible for the reduction of sizes of foliated particles, which abrade at about 10 times the rate of non-foliated particles.



## **ACKNOWLEDGMENTS**

This work was supported through a cooperative agreement with the USDA Forest Service, Pacific Northwest Research Station, administered through Dennis Harr. Additional research funds came from the Western Washington University geology department and a graduate student research grant from the Geological Society of America. The Campbell Group (David Chamberlain) and Crown Pacific (Norm Schaaf) provided access to the field area.

I thank my committee members Harvey Kelsey, Christopher Suczek and Russell Burmester for their encouragement, critical thinking and timely reviews of products. Harvey is a model of energy and professionalism, and I am privileged to have worked with him. Chris always made herself available for reviews, and she provided constant encouragement. Russ has the unique ability to dissect a problem, investigate the individual components, and construct a solution, all without losing sight of the big picture.

Special thanks go to John O'Leary, who assisted me in the field, and who constantly and constructively challenged my methodology and interpretations. JoAnn Holloway, Aundrea Noffke and Kris Alvarez also assisted; thank you all very much. Thanks also to Jeff Kirtland for our many discussions, and to Kirk Stephens and Duane Olson for a brief retreat chasing little white balls and clubbing them.

George Mustoe provided tremendous assistance in the design of the abrasion tank and the procurement of its materials. Chris Sutton and Vicki Critchlow were beacons of light in the often dark seas of administrative requirements.

My entire graduate endeavors would not have been possible without the support, commitment and ever-lasting patience of my loving family; thank you Lydia, Kayla and Will. Thank you Mom, Bill and Mary.



## TABLE OF CONTENTS

|  |    |
|--|----|
| ABSTRACT .....   | i  |
| ACKNOWLEDGMENTS .....  | ii |
| LIST OF FIGURES.....   | v  |
| LIST OF TABLES.....  | vi |
| INTRODUCTION.....  | 1  |
| STUDY AREA .....   | 4  |
| SAMPLING PROCEDURES: .....   | 9  |
| Particle Size and Particle Lithology .....   | 9  |
| Particle Shape .....   | 10 |
| DOWNSTREAM FINING TRENDS.....  | 14 |
| DOWNSTREAM FINING TRENDS VERSUS SIZE AND ABUNDANCE OF<br>CLASTS OF DIFFERENT LITHOLOGY .....   | 19 |
| CHANGES IN PARTICLE SHAPE WITH FINING:.....  | 25 |
| Sphericity versus Fining .....   | 25 |
| Changes in Clast Form versus Fining .....  | 25 |
| ABRASION TANK STUDY .....  | 29 |
| DISCUSSION:.....   | 33 |
| Finning Trends and Coarse Sediment Input from Debris Flows and<br>Debris Slides .....          | 33 |
| Insights Into Fining Mechanisms for Particles Less Than 400 mm<br>Field Data.....              | 36 |
| Particle Shape Changes with Downstream Changes in Particle Size<br>Field versus Tank Data..... | 37 |



Combining Tank and Field Data

Approximating the Separate Contributions of Abrasion and

Sorting Processes to Fining Mechanisms ..... 38

SUMMARY ..... 44

REFERENCES ..... 46

APPENDIX ..... 49

## LIST OF FIGURES

|            |   |    |
|------------|---|----|
| Figure 1.  | Location map and geology of the Finney Creek study basin .....  | 3  |
| Figure 2.  | Map showing sample locations in the Finney Creek study reach .....  | 6  |
| Figure 3.  | Cumulative grain size distributions .....   | 11 |
| Figure 4.  | Sphericity-form diagram of Sneed and Folk (1958) .....  | 13 |
| Figure 5.  | Median D100, D90 and D50 grain size versus distance .....   | 15 |
| Figure 6.  | Best-fit regression curves for D100, D90 and D50 grain size in four fining reaches .....  | 16 |
| Figure 7.  | Grain size and abundance versus distance for foliated and non-foliated rock types of the D100 .....   | 21 |
| Figure 8.  | Mean grain size and abundance versus distance for 12 largest foliated and non-foliated rock types from the D100.....                                  | 23 |
| Figure 9.  | Shapes of foliated and non-foliated particles measured in fining Series 1 and 3, plotted on the sphericity-form diagram of Sneed and Folk (1958)..... | 27 |
| Figure 10. | Shapes of foliated and non-foliated particles used in the experiment of abrasion plotted on the sphericity-form diagram of Sneed and Folk (1958)..... | 31 |
| Figure 11. | Comparison of particle fining trends for partially buried and fully exposed particles in fining Series 1 and 3 .....                                  | 35 |
| Figure 12. | Plot of grain sizes of particles transported in the abrasion tank .....   | 40 |
| Figure 13. | Plots of predicted D100 grain size versus distance in fining Series 1, considering the separate effects of abrasion and selective transport .....     | 41 |
| Figure 14. | Schematic drawing of the abrasion tank .....  | 50 |

## LIST OF TABLES

|          |  |    |
|----------|--|----|
| Table 1. | Drainage-basin characteristics of the Finney Creek study basin .....   | 5  |
| Table 2. | Distribution of geologic units within the Finney Creek study basin .....                                     | 7  |
| Table 3. | Variables for curve-fitting for downstream fining trends, Finney Creek .....                                 | 17 |
| Table 4. | Principle lithologies of the 51 largest particles measured at 43 sites in the Finney Creek Study reach ..... | 20 |
| Table 5. | Variables for curve-fitting for downstream fining trends of two rock types of the D100 size class.....       | 22 |
| Table 6. | Data on particle shapes from the first and last sample locations of Series 1 and Series 3.....               | 26 |
| Table 7. | Abrasion tank data on size and shape .....   | 30 |



## INTRODUCTION

Particles tend to fine in the downstream direction. Previous studies have documented trends of fining in natural gravel-bed rivers (Bradley, 1970; Bradley et al., 1972; Brierly and Hicken, 1985; Church and Kellerhals, 1978; Knighton, 1980; Werrity, 1992). While the studies show overall fining trends, scatter about a regression can be attributed to contributions of new material at tributary junctions and from channel banks (Church and Kellerhals, 1978; Knighton, 1980) and to the differential effects of abrasion on contrasting lithologies in transported sediment loads (Knighton, 1980; Werrity, 1992).

Abrasion and selective transport are two sets of processes commonly accepted as explanations for observed fining trends. Abrasion is a summary term for mechanical processes of diminution by cracking, splitting, chipping and grinding. Progressive downstream sorting by selective transport results from flow competence. The relative importance of abrasion and selective transport processes, and how they vary with variation in particle sizes, shapes, and lithologies, are still incompletely understood. Experimental and field studies have attested to the effectiveness of abrasion (Bradley, 1970; Krumbein, 1941; Shaw and Kellerhals, 1982; Werrity, 1992), while other studies concluded that selective transport is an effective mechanism producing downstream fining and may be more effective than abrasion in streams with abundant sediment supply (Bradley et al., 1972; Brierly and Hicken, 1985; Paola et al., 1992).

Few studies have investigated particle fining in mountain streams in which channels are supplied with an abundance of sediment. In alluvial channels of mountain streams in the Pacific Northwest, the spatial and temporal distribution of particles is affected by debris flows (Benda, 1989). These channels provide an opportunity to investigate the phenomenon of particle fining because the volume of poorly sorted sediment that is episodically delivered directly to stream



channels from adjacent hillslopes by debris flows may initially exceed the sediment transport capacity of the stream. Consequent changes to the distribution of particle sizes in the channel downstream of a debris deposit must be attributable to either selective transport or abrasion, or to a combination of both processes.

This study investigates the downstream decrease in grain size (fining) of the largest particles in a mountain stream channel with recent debris-flow input, and investigates whether fining is related to contributions of coarse clasts from debris flows. The study also investigates the relation of particle fining to particle lithology and particle shape. Finally, the relative importance of abrasion and selective transport as a fining mechanism is evaluated .

The site selected for this study is Finney Creek, a third-order tributary to the Skagit River in northwest Washington (Figure 1). The studied channel drains mountainous terrain of the west slopes of the North Cascade range. The channel was sampled systematically to provide an inventory of the largest clast sizes, lithologies and shapes. All reaches were investigated for the occurrence of debris deposits. Field sampling and laboratory investigations were performed during the summers of 1992 and 1993.

The purpose of this study is three-fold: 1) determine if there is any systematic distribution of the largest particles in mountain stream channels; 2) analyze the controls on trends of particle fining with respect to debris-flow history, source-area lithology and rock durability; and 3) assess the roles of selective transport and abrasion in producing the observed trends of particle fining.



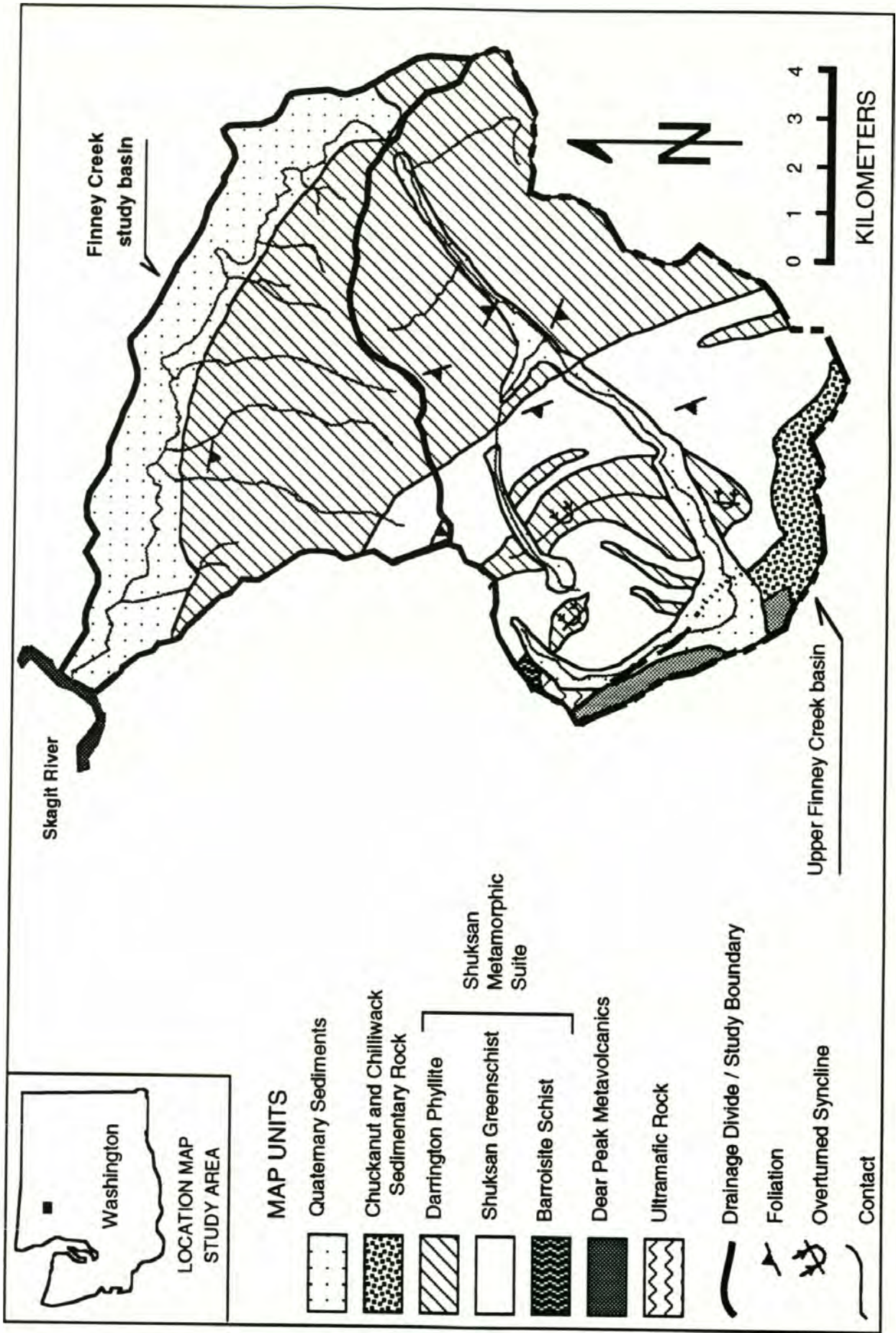


Figure 1. Location map and geology of the Finney Creek study basin.



## STUDY AREA

Finney Creek drains mountainous terrain of the western slopes of the Cascade Range in northwest Washington (Figure 1). The Finney Creek drainage area comprises 134 km<sup>2</sup> of rugged, heavily forested land south of the Skagit River. Relief within the entire basin is greater than 1400 meters (Table 1), and the majority of hillslopes exceed 25 degrees. The location and age of recent debris-slide and debris-flow deposits and the location of small stream-side mass movements in the Finney Creek study reach are shown in Figure 2. Slide deposits were identified in the field and assigned ages of deposition based on field evidence and aerial photo interpretation.

Climatologic, lithologic and structural characteristics within the basin contribute to active landslide processes. High annual precipitation and rain-on-snow precipitation events affect slope stability in the basin (Parks, 1992). Rain-on-snow events in the basin also have produced rapid fluctuations of discharge (Harr et al., 1989). Annual precipitation averaged 1730 mm/yr from 1931 to 1991 (National Climatic Data Center, 1991) at a U.S. Weather Service observation station that is located 18 km north of Finney Creek in the town of Concrete, at an elevation of 61 m. The stream is not presently gaged, although some flow data for water years 1943 to 1948 are available. Streamflow values ranged from a minimum daily discharge of 0.55 m<sup>3</sup> sec<sup>-1</sup> to a maximum daily discharge of 83 m<sup>3</sup> sec<sup>-1</sup> (U.S.G.S., 1943 to 1948). The two-year bankfull discharge, calculated at the downstream end of the drainage basin using a regression equation and exponents specific to Region I of western Washington (Cummins et al., 1975), is 144 m<sup>3</sup> sec<sup>-1</sup>.

The Finney Creek basin is underlain almost entirely by the Cretaceous and Jurassic Shuksan Metamorphic Suite (Figure 1 and Table 2), which includes metabasaltic greenschist with some intercalated blueschist, and quartzose -

TABLE 1: Drainage-Basin Characteristics For The Finney Creek Study Basin

|   | Finney Creek |             |
|---|--------------|-------------|
|   | Entire basin | Study reach |
| Drainage area (km <sup>2</sup> )                          | 134          | 55          |
| Basin relief (m)  | 1489         | 1365        |
| Aspect  | SE - SW      | N - NE      |
| Stream order  | third        | third       |
| Average channel gradient                                  | 0.034        | 0.0064      |
| Average unvegetated channel width (m)                     | >25          | 31          |
| Two - year discharge* (m <sup>3</sup> sec <sup>-1</sup> ) | 144          | --          |

\* Discharge with a recurrence interval of two years, calculated based on drainage area and annual precipitation using regression relations of Cummins et al. [1975]. Calculated for entire basin at distal end of study reach near the confluence with Skagit River.



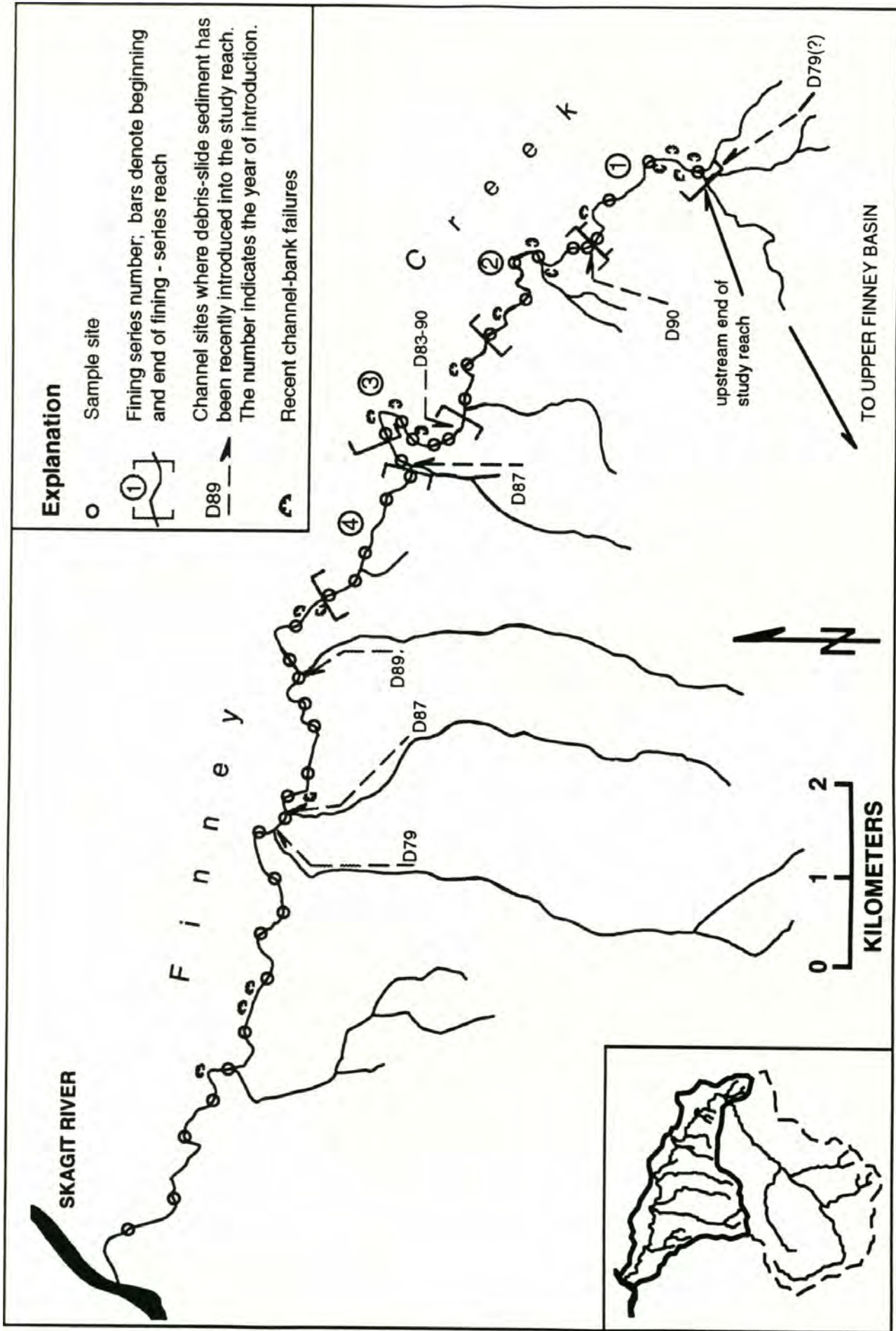


Figure 2. Finney Creek study area showing study reaches, sample locations, recent channel-bank failures and channel sites where sediment from debris flow has been introduced recently into the study channel.



TABLE 2: Distribution of Geologic Units Within The Finney Creek Study Basin

| Rock unit*                                 | Finney Creek    |            |                 |            |
|--|-----------------|------------|-----------------|------------|
|  | Entire basin    |            | Study reach     |            |
|  | km <sup>2</sup> | % of basin | km <sup>2</sup> | % of basin |
| Quaternary sediments                       | 29              | 22         | 22              | 40         |
| Darrington phyllite                        | 70              | 52         | 31              | 56         |
| Shuksan greenschist                        | 31              | 23         | 2               | 4          |
| Barroisite schist                          | <1              | <1         | --              | --         |
| Deer Peak metavolcanics                    | 2               | ~1         | --              | --         |
| Chilliwack and Chuckanut sedimentary rocks | 2               | ~1         | --              | --         |
| Ultramafic rocks                           | <1              | <1         | --              | --         |

\* From Brown et al., 1987

carbonaceous phyllite (Brown et al., 1987). Small areas in the extreme upper basin include ultramafic rock, Mesozoic metavolcanics and Tertiary sandstone. The predominant structural element in the Shuksan Metamorphic Suite in this area is a foliation that strikes northwest and dips steeply to the southwest (Brown et al., 1987). The basin has been extensively glaciated, and surficial deposits of till, outwash and lacustrine material mantle the bedrock throughout the area.

The study reach is in the lower 40% of the Finney Creek basin. The upstream end of the Finney Creek study reach (Figure 2) commences where Finney Creek emerges from a bedrock canyon that also defines the upstream limit of anadromous fish passage, and extends 20.4 km downstream to within one km of the confluence with Skagit River (Figure 2). The channel has an irregular pattern, and it is generally confined by its valley walls. In the study reach, Finney Creek flows primarily on alluvial cobble; exposures of bedrock in the channel are rare.

Phyllite bedrock and Quaternary sediments are the major map units represented in the Finney Creek study basin (Figure 1, Table 2). The fissile, platy character of much of the phyllite unit makes it highly prone to mass failure. A landslide inventory for the entire Finney Creek watershed has documented that slope failures occur most frequently as debris slides in that portion of the basin underlain by phyllite bedrock (Parks, 1992). The Quaternary sediments are part of the Skagit River valley fill deposited during the last glaciation (ca. 18 - 14 ka [Thorson, 1989]). The valley fill makes up the hilly terrain that confines Finney Creek on its north bank within the study reach (Figure 1).



## **SAMPLING PROCEDURES: PARTICLE SIZE, PARTICLE LITHOLOGY AND PARTICLE SHAPE**

### Particle Size and Particle Lithology

The first objective of the study was to determine whether particle sizes systematically changed downstream. Sample sites were selected based on a systematic sampling strategy (Krumbein and Graybill, 1965; Smartt and Granger, 1974). The channel was divided into segments between confluences shown by intersections of blue lines on a 1:24,000 topographic map, and sample sites were mapped at equally spaced intervals within each segment. In the field, a systematic search was undertaken to locate the largest size particles on the coarsest surface of the active channel bar nearest each mapped site. Generally, the largest sizes were found either at the head of the bar or close to the active channel. Typically, the length of bar sampled was between 80 and 100 m. Sampling of particle sizes was performed on a total of 43 sites at an average interval of about 15 channel widths (Figure 2). A closer spacing of sample sites was warranted in some channel segments where recent debris slides had deposited sediment (Figure 2).

Downstream fining was examined as the trend in the largest clast sizes, using field procedures adopted from Bradley et al. (1972) and Werrity (1992). The apparent intermediate axis (b-axis) was measured on at least the 51 largest particles that could be found at a site, and the rock type of each of the measured clasts was recorded. On average, between 65 and 70 particles were selected at each sample site. The lengths of the intermediate axes were then ranked and, using the 51 largest clasts for each sample site, the median b-axis diameter was computed. This median of particle sizes will henceforth represent the largest size class of particles and will be referred to as the D100. Sizes reported from these measures are minimums due to partial burial of some particles.



After measurement of the largest particles, a Wolman (1954) pebble count was performed over the coarsest section of the bar. The line of measurement was oriented parallel with stream flow. The purposes of the count were to record the intermediate diameters of particles in half-phi size units and to do an inventory of all clasts by lithology, not just for the D100 clasts. The D90 and D50 particle sizes were derived from cumulative frequency analysis of the particle-size data collected (Figure 3).

### Particle Shape

Particle size and lithology are the dominant variables that control changes in sphericity and form (Sneed and Folk, 1958), and particle sphericity and form are two components of particle morphology that have been demonstrated to affect a particle's resistance to fluvial transport (Bradley, 1970; Bradley, et al., 1972; Krumbein, 1941 and 1942; Sneed and Folk, 1958). When transported by traction, the velocities of spherical particles exceed the velocities of disc-shape particles of the same mass (Krumbein, 1942), though that is not necessarily the case with particles of the same size (b-axis) but with different mass (Bradley, 1972, and references therein).

Particle sphericity is a measure of how nearly the shape of a particle approaches that of a sphere. Therefore, an appropriate measure of sphericity of a particle is the ratio of the maximum projection area of a sphere of the same volume as the particle to the maximum projected area of the particle. The ratio is called the *maximum projection sphericity*,  $\Psi$ , where

$$\begin{aligned}\Psi &= \pi/4 [(abc)^{1/3}]^2 + \pi/4 (ab) \\ &= [c^2 + (ab)]^{1/3}\end{aligned}$$

and a, b and c are the long, intermediate and short axes of the particle (Sneed and Folk, 1958).



Figure 3. (Upper) Cumulative grain-size distributions derived by the Wolman (1954) pebble-count method for the 43 samples collected within the Finney Creek study reach. (Lower) Cumulative grain-size distributions for the four fining series. Dashes are extrapolated extensions of grain-size curves for those sites where an upper limit on clast size was imposed during field measurements.

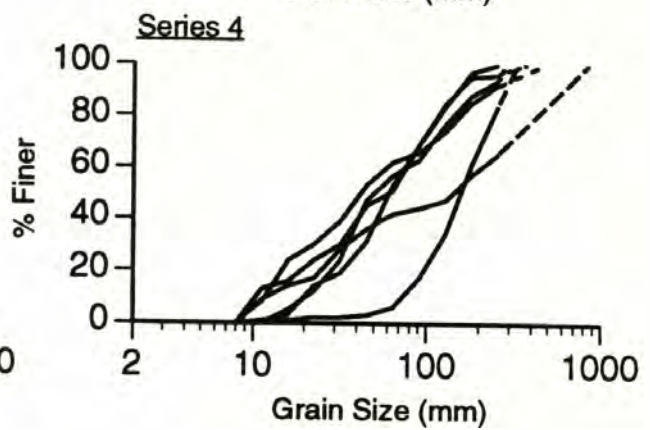
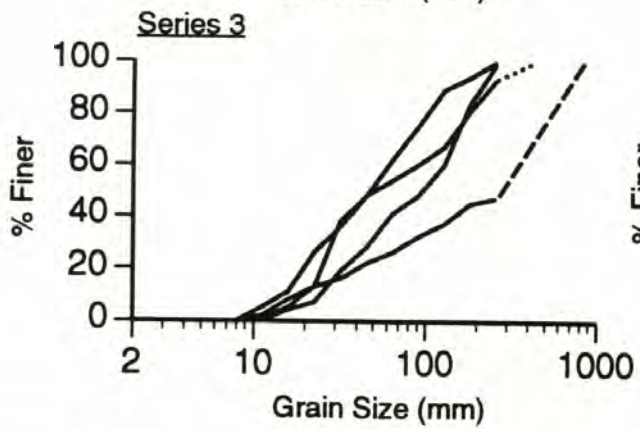
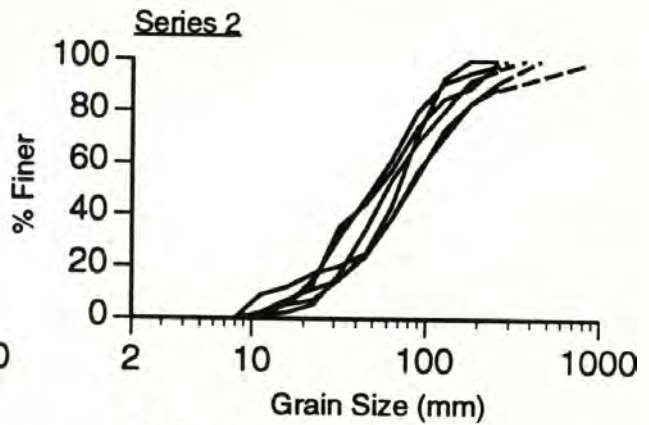
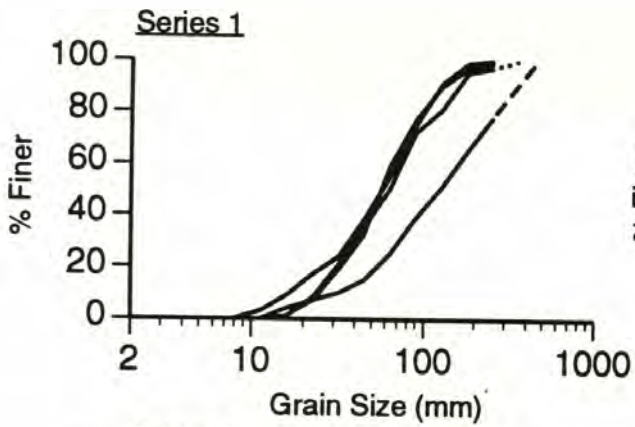
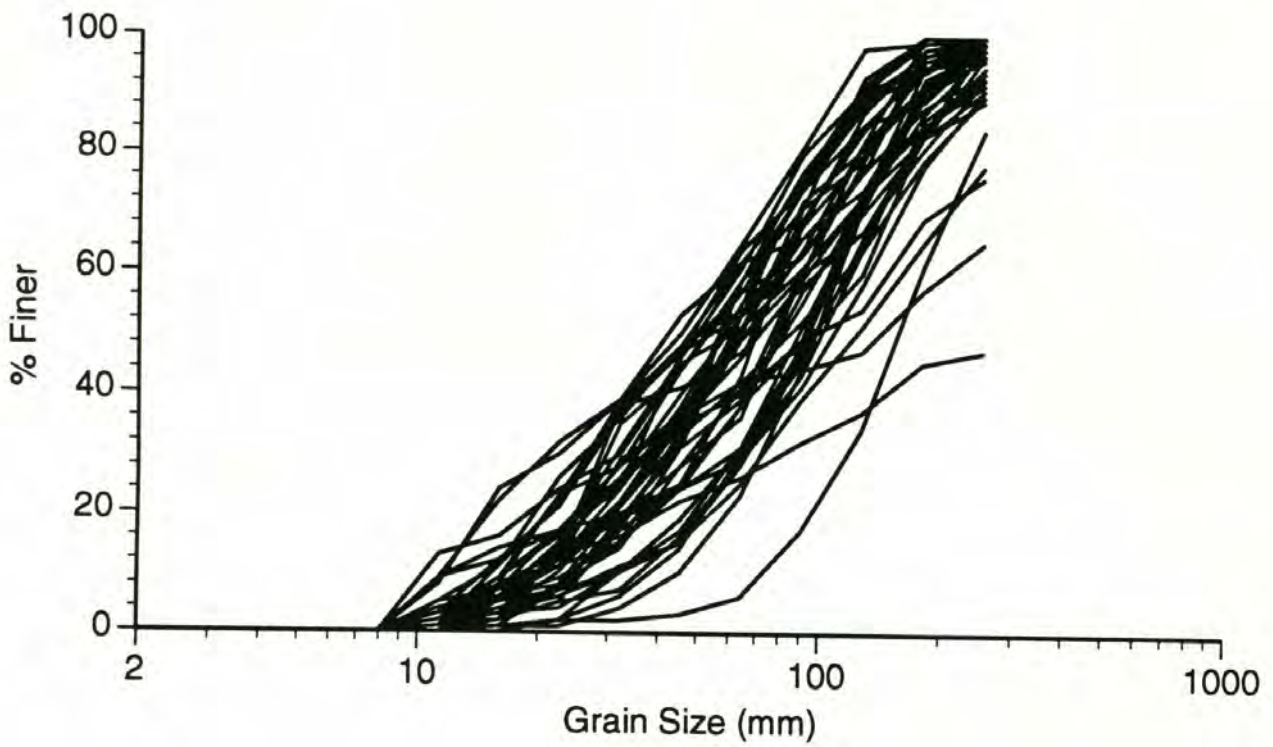


Figure 3



Particles of the same sphericity may have different ratios between their three dimensions. Form is a measure of the relation between the three dimensions of a particle. Particles may be classified quantitatively as compact (equidimensional), elongate (rodlike), bladed, or platy (disclike), with a range of intermediate categories (Figure 4). In studying the effects of shape on transport, analysis of both form and maximum projection sphericity is better than analysis of sphericity alone (Sneed and Folk, 1958).

Particle shapes (sphericity and form) were determined for fully exposed particles of D100 size. Only fully exposed particles were chosen so that all three principle axes could be measured. Particle shape measurements were performed after sampling the entire study reach for size and lithology. In this way, particle shape analysis focused on stream reaches where particle-fining trends were documented.

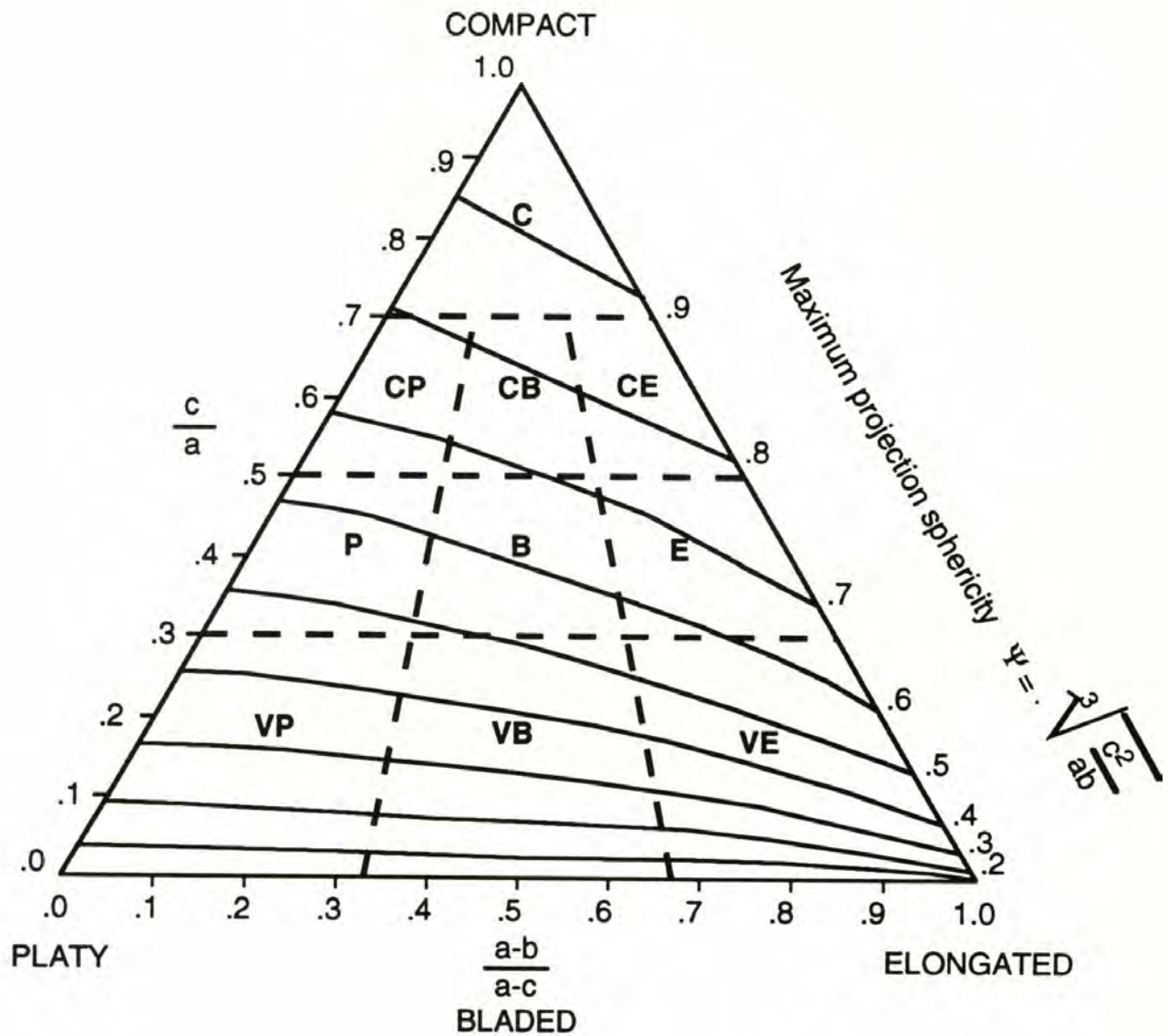


Figure 4. The sphericity-form diagram of Sneed and Folk (1958). Given the long (a), intermediate (b) and short (c) axial measures of a particle or mean of sample particle lengths, particle form is determined by plotting the two diameter ratios  $c/a$  and  $(a-b) / (a-c)$ . Ten form classes are defined by the dashed lines: C, compact; CP, compact-platy; CB, compact-bladed; CE, compact-elongate; P, platy; B, bladed; E, elongate; VP, very platy; VB, very bladed; VE, very elongate.



## DOWNSTREAM FINING TRENDS

Particle-size versus distance downstream (Figure 5) shows marked changes where some debris deposits and tributary junctions are located. These particle-size changes serve as a basis for breaking the channel into two zones and for breaking the upper zone into four data series. The lower 10 km of the channel shows no apparent trend with regard to particle-size, whereas in the upper 10 km, four separate data series (henceforth called Series 1, Series 2, Series 3 and Series 4) each define a trend of decreasing grain size with distance downstream. The spike in grain size that defines the start of each series is spatially associated with a recent debris flow deposit or debris slide deposit in the channel (shown by the up arrows on the longitudinal profile in Figure 5). In two of the four cases, associated debris flows were routed through tributaries; the locations of tributaries are shown as down arrows in Figure 5.

The four trends of reduction in grain size were assessed with respect to distance downstream from each spike in order to evaluate whether grain size decreased exponentially, and whether the trend was better defined by the D100, D90 or D50 grain sizes. Figure 6 graphically presents the four series of grain-size reduction as log-linear plots. In each series, distances over which fining occurs are adjusted so that zero distance for each series is at the start of the series. Within each graph, regression lines for an exponential function are fitted through the D100, D90 and D50 grain size percentiles (Figure 6). An incomplete data set hampers the analysis for Series 3, a reach consisting of a bedrock gorge in phyllite. Here, the D90 and D50 size classes were not measured at the first sampling site.

Table 3 shows the variables for the best-fit relations between grain size and channel length (Figure 6) for the channel reaches over which trends of reduction in grain size were found. In comparing the  $r^2$  values for the best-fit

Figure 5. (Upper) Median D100 grain size versus distance for the entire Finney Creek study reach. Four series of fining trends are depicted for the three different size classes. (Lower) Longitudinal profile of the Finney Creek study reach. Arrows directed down show tributary junctions; arrows directed up show locations of recent debris deposits in the channel.



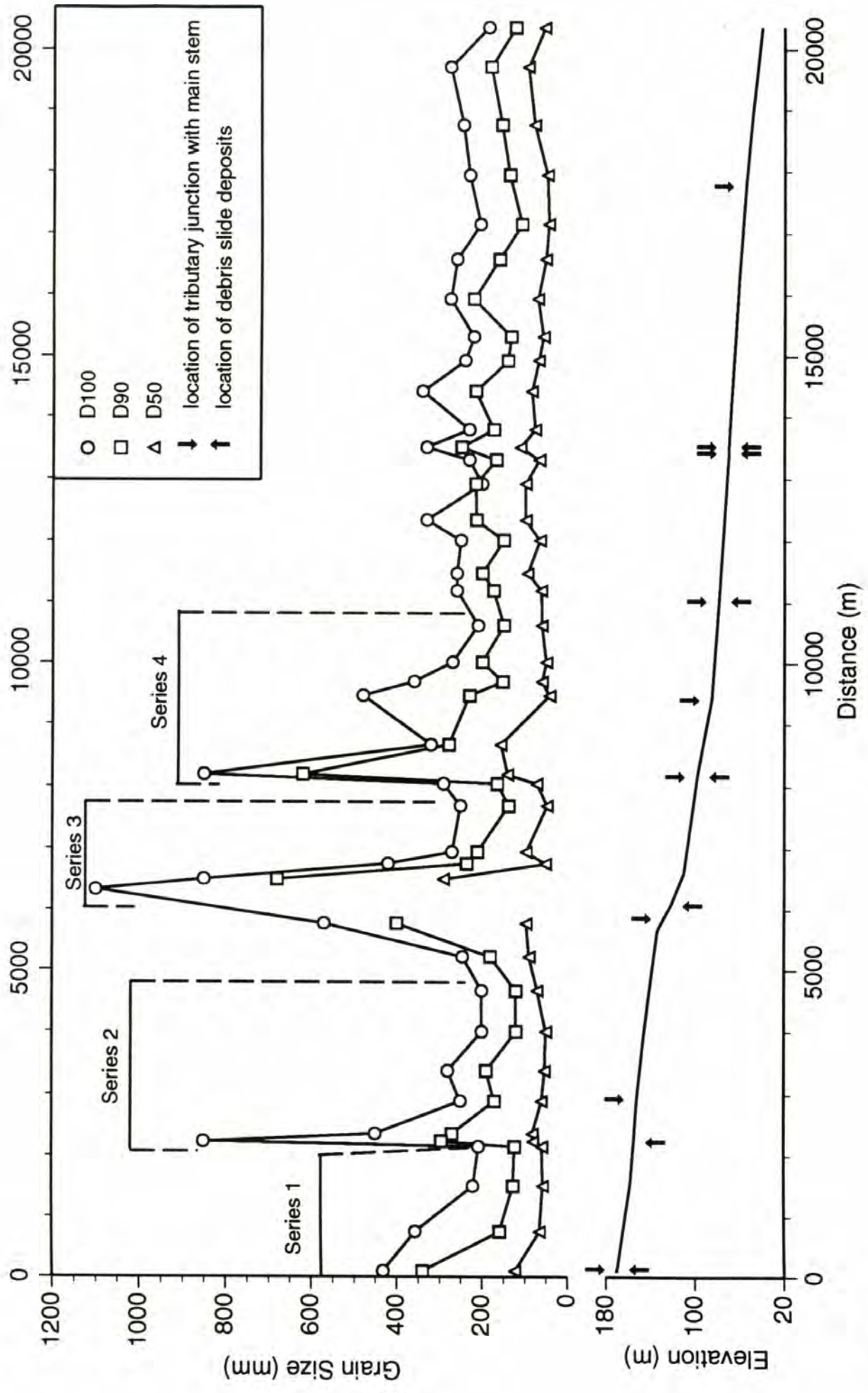


Figure 5

Figure 6. Four series of fining trends plotted on log-linear scale for the D100, D90 and D50 size classes. Best-fit regression lines for an exponential function fit to the data are shown for each size class in each series. For the regression analysis, distance is normalized to the start of each series. Symbols are the same as in Figure 5.



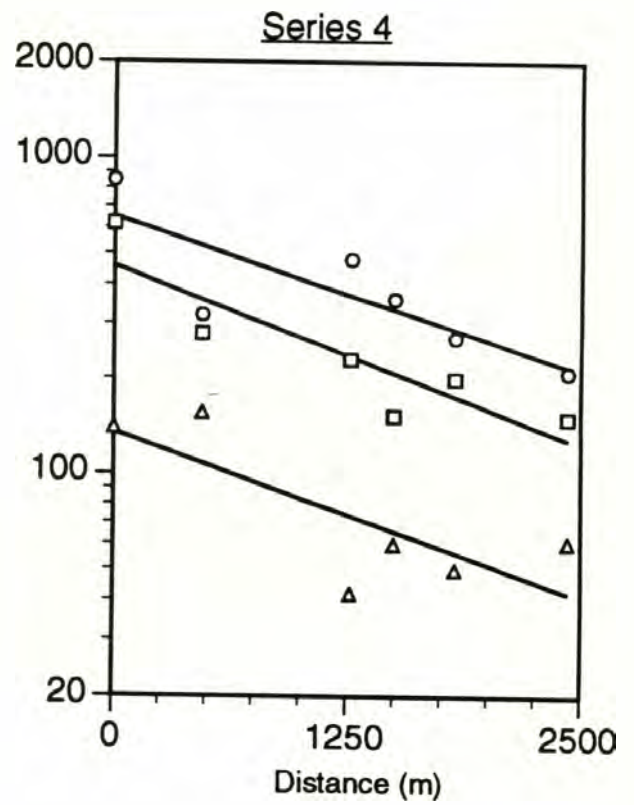
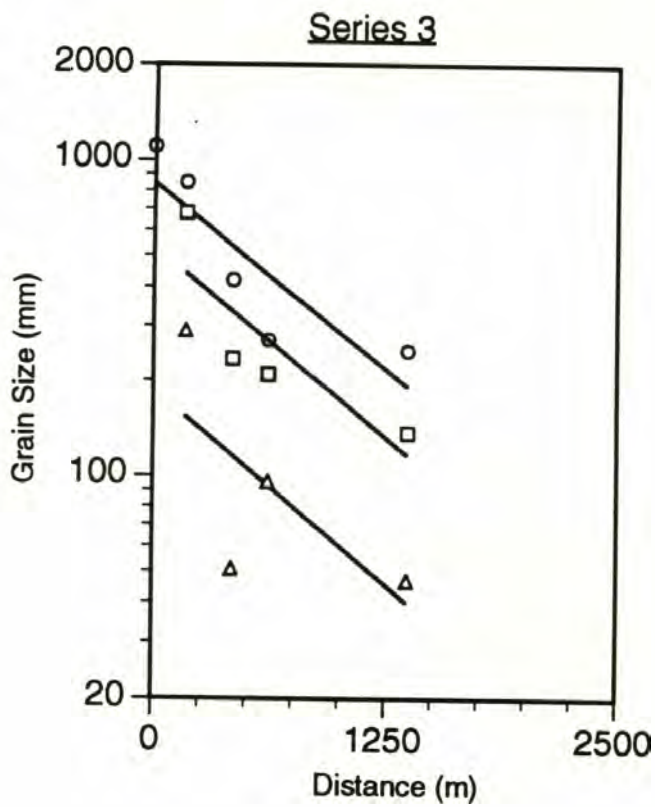
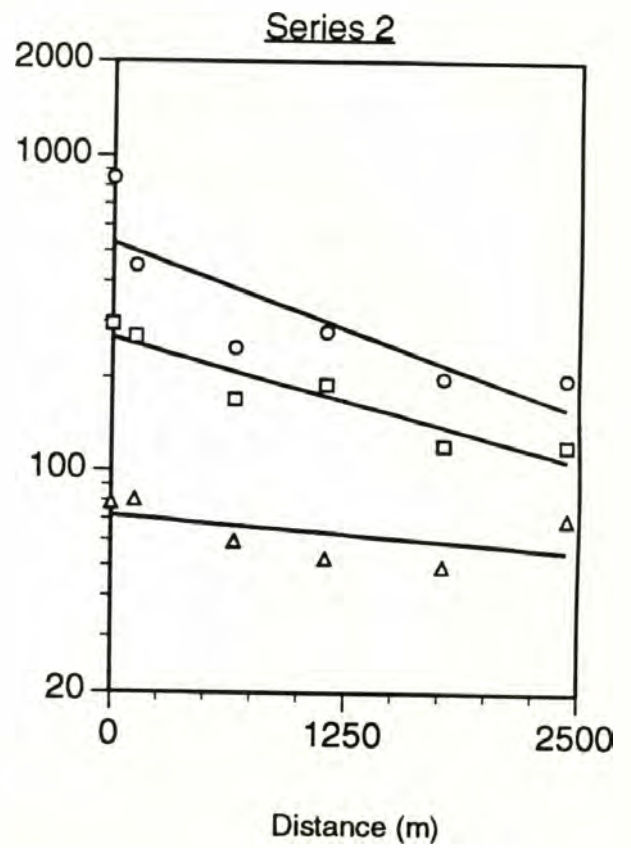
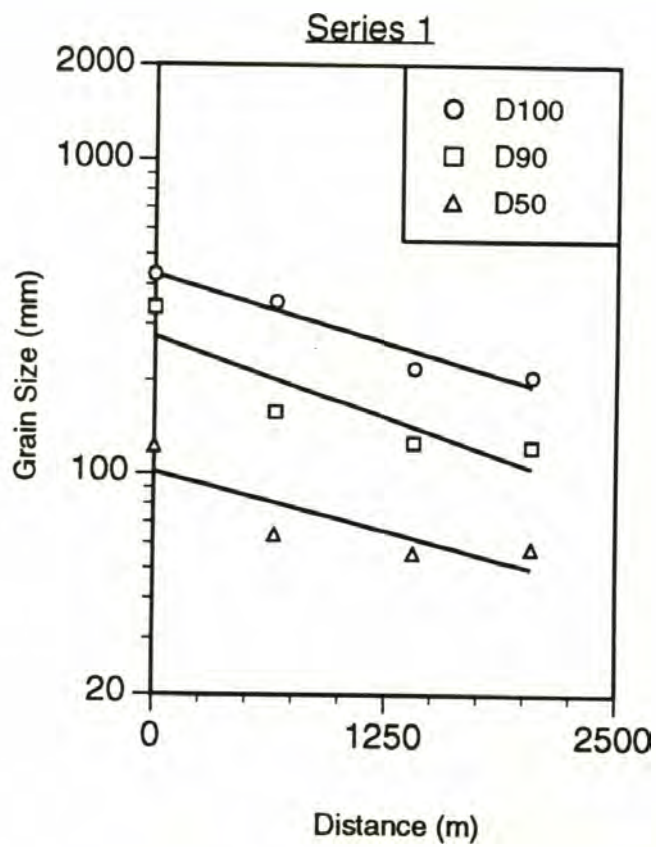


Figure 6

TABLE 3: Variables For Curve Fitting For Downstream Fining Trends, Finney Creek

| Particle size class | Downstream fining series | Length of channel, L (m) | Exponential fit: $y=be^{ax}$ ,<br>a=slope; b=intercept;<br>$y=D100(\text{mm})$ ;<br>x = distance downstream (meters) |           |  |                |
|---------------------|--------------------------|--------------------------|--|-----------|--|----------------|
|                     |                          |                          | intercept (b) (mm)   | slope (a) | fining coefficient a ( $\text{km}^{-1}$ )* | r <sup>2</sup> |
| <b>D 100</b>        | Series 1                 | 2040                     | 430  | -0.00039  | -0.39                                      | 0.94           |
|                     | Series 2                 | 2430                     | 530  | -0.00049  | -0.49                                      | 0.70           |
|                     | Series 3                 | 1370                     | 850  | -0.00110  | -1.10                                      | 0.74           |
|                     | Series 4                 | 2430                     | 650  | -0.00045  | -0.45                                      | 0.67           |
| <b>D 90</b>         | Series 1                 | 2040                     | 280  | -0.00048  | -0.48                                      | 0.79           |
|                     | Series 2                 | 2430                     | 270  | -0.00038  | -0.38                                      | 0.87           |
|                     | Series 3                 | 1370                     | 440  | -0.00110  | -1.10                                      | 0.72           |
|                     | Series 4                 | 2430                     | 460  | -0.00053  | -0.53                                      | 0.79           |
| <b>D 50</b>         | Series 1                 | 2040                     | 101  | -0.00035  | -0.35                                      | 0.69           |
|                     | Series 2                 | 2430                     | 72   | -0.00011  | -0.11                                      | 0.25           |
|                     | Series 3                 | 1370                     | 150  | -0.00110  | -1.10                                      | 0.48           |
|                     | Series 4                 | 2430                     | 140  | -0.00048  | -0.48                                      | 0.60           |

\* the fining coefficient (Paola et al., 1992) is an empirical factor that relates percentile class size to distance downstream ( $\% + 1000\text{m}$ ) or  $\text{km}^{-1}$



relations in Figure 6, particle size reductions are best described for the D100 and D90 size classes and least well described for the D50 size class. In Series 1 and Series 3, the strength of the exponential function as a predictor of grain-size reductions increases through the particle size range, being greatest for the D100 size class and least for the D50 size class.

While fining trends are clearly well defined for both the D100 and D90 particle size classes, subsequent analysis of particle lithology and particle shape will be restricted to only the D100 size class. The method for identifying the D100 was easy to apply in the field, and the coarsest fraction represents particle sizes that are most likely to challenge Finney Creek's competence.

## **DOWNSTREAM FINING TRENDS VERSUS SIZE AND ABUNDANCE OF CLASTS OF DIFFERENT LITHOLOGY**

Lithologies recorded during the survey of D100 clasts reveal that they fall in two groups. All of the largest particles measured in the channel (Table 4) appear to be phyllite or from the Quaternary unit (Table 2). Particles in the Quaternary unit are dominantly comprised of hard igneous and hard metavolcanic rock (Table 4). These particles are massive and rounded to very well-rounded. The shapes of particles from this unit appear to be inherited from exogenous factors related to glacial erosion processes. Rock types in the Quaternary unit can reasonably be classified as non-foliated in comparison to the phyllite clasts, which are foliated. The along-channel distribution and size of particles belonging to these two groups provides a basis for assessing rates of particle-size reduction and abundance between foliated and non-foliated rock of the largest size class.

Results of grain-size analysis by rock type (foliated vs. non-foliated) plotted against distance downstream for the four fining series (Figure 7) suggest that fining trends are essentially equivalent for both rock-type classes. However, at many of the sites phyllite comprises a small fraction of the sample pool of largest size rocks, and in a few sample locations none of the 51 largest particles is phyllite (bottom, Figure 7).

To better assess comparative fining trends for foliated versus non-foliated particles, the reaches that encompass Series 1 and Series 3 were re-examined for particle lithology and particle shape. Only fully exposed D100 particles were tallied for lithologic types (foliated or non-foliated) and at least 12 largest clasts for each rock type were measured at each site. Sizes were calculated as the mean of the 12 largest particles of each rock type. Results are summarized in



TABLE 4: Principle Lithologies Of The 51 Largest Particles Measured at 43 Sites In The Finney Creek Study Reach

| Classification | Rock type  | % of total |
|----------------|--|------------|
| Foliated       | Phyllite   | 17.5       |
| Non-foliated   | Igneous<br>Includes granite, diorite,<br>gabbro, andesite and basalt                             | 58.3       |
|                | Metamorphic<br>Includes metavolcanic,<br>metaconglomerate, quartz,<br>ultramafic and greenstone* | 24.2       |

\* Although the source of some of the greenstone may be the Shuksan greenschist unit in the upper Finney Creek basin, none of these largest particles exhibited a foliated texture.

Figure 7. (Upper) Median grain size versus distance downstream for foliated (open squares), non-foliated (open triangles) and combined (open circles) rock types of the D100, plotted for all four fining series. (Lower) Abundance of foliated (phyllite) and non-foliated (clasts derived from Quaternary unit) clasts at each sample site in the four fining series.



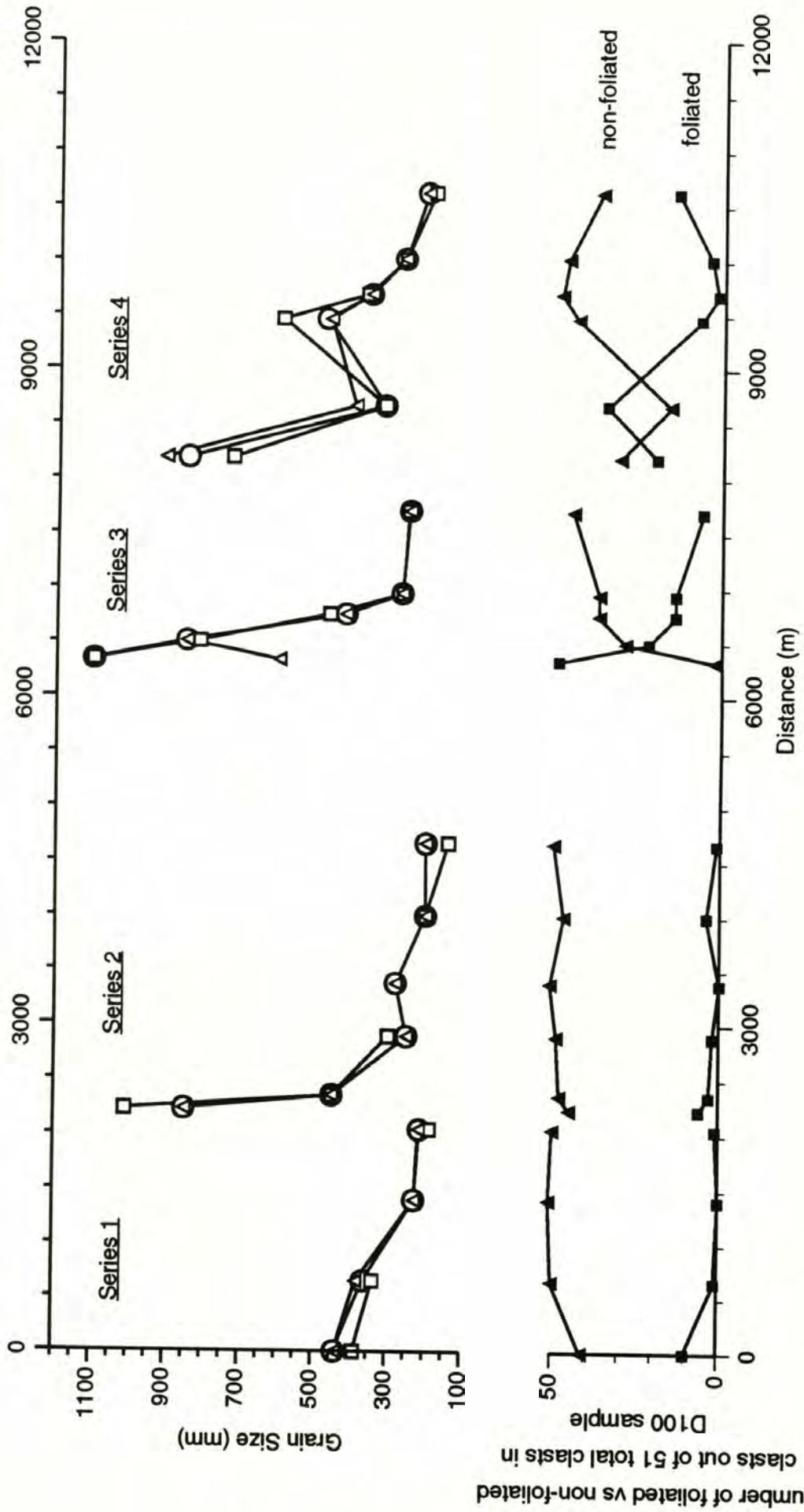
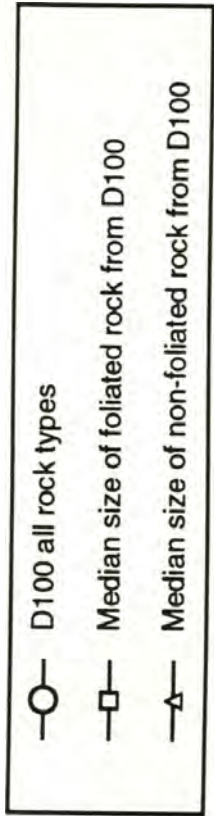


Figure 7

TABLE 5: Variables For Curve Fitting For Downstream Fining Trends of Two Rock-Types of The D100 Size Class

| Downstream fining series | Rock type *             | Length of channel, L (meters) | Exponential fit: $y=be^{ax}$                        |           |   |      |
|--------------------------|-------------------------|-------------------------------|---|-----------|---|------|
|                          |                         |                               | intercept (b) (mm)                                  | slope (a) | fining coefficient (1000)a (km <sup>-1</sup> )† |      |
|                          |                         |                               | $y=D100$ (mm);<br>$x=$ distance downstream (meters) |           |   |      |
|                          |                         |                               | $r^2$   |           |   |      |
| Series 1                 | D100 combined           | 2040                          | 374   | -0.00033  | -0.33   | 0.99 |
|                          | 12 largest foliated     | 2040                          | 364   | -0.00040  | -0.40   | 0.90 |
|                          | 12 largest non-foliated | 2040                          | 455   | -0.00029  | -0.29   | 0.88 |
| Series 3                 | D100 combined           | 1370                          | 547   | -0.00073  | -0.73   | 0.82 |
|                          | 12 largest foliated     | 1370                          | 953   | -0.00124  | -1.24   | 0.82 |
|                          | 12 largest non-foliated | 1370                          | 405   | -0.00020  | -0.20   | 0.19 |

\* D100 = median of 51 largest particles; 12 largest foliated and 12 largest non-foliated = mean of 12 largest of each rock type.

† the fining coefficient has units of km<sup>-1</sup> because it is an empirical factor that relates percentile class size to distance downstream (% + 1000m).



Figure 8. A, Downstream fining trend for D100 clasts (median of 51 fully exposed clasts only). B, Downstream abundance of clasts of different lithology. C, Downstream fining trends for clasts of different lithology (mean size of 12 largest fully exposed clasts of each lithology).

○ D100 of 51 fully exposed    □ Mean size of 12 largest foliated    △ Mean size of 12 largest non-foliated

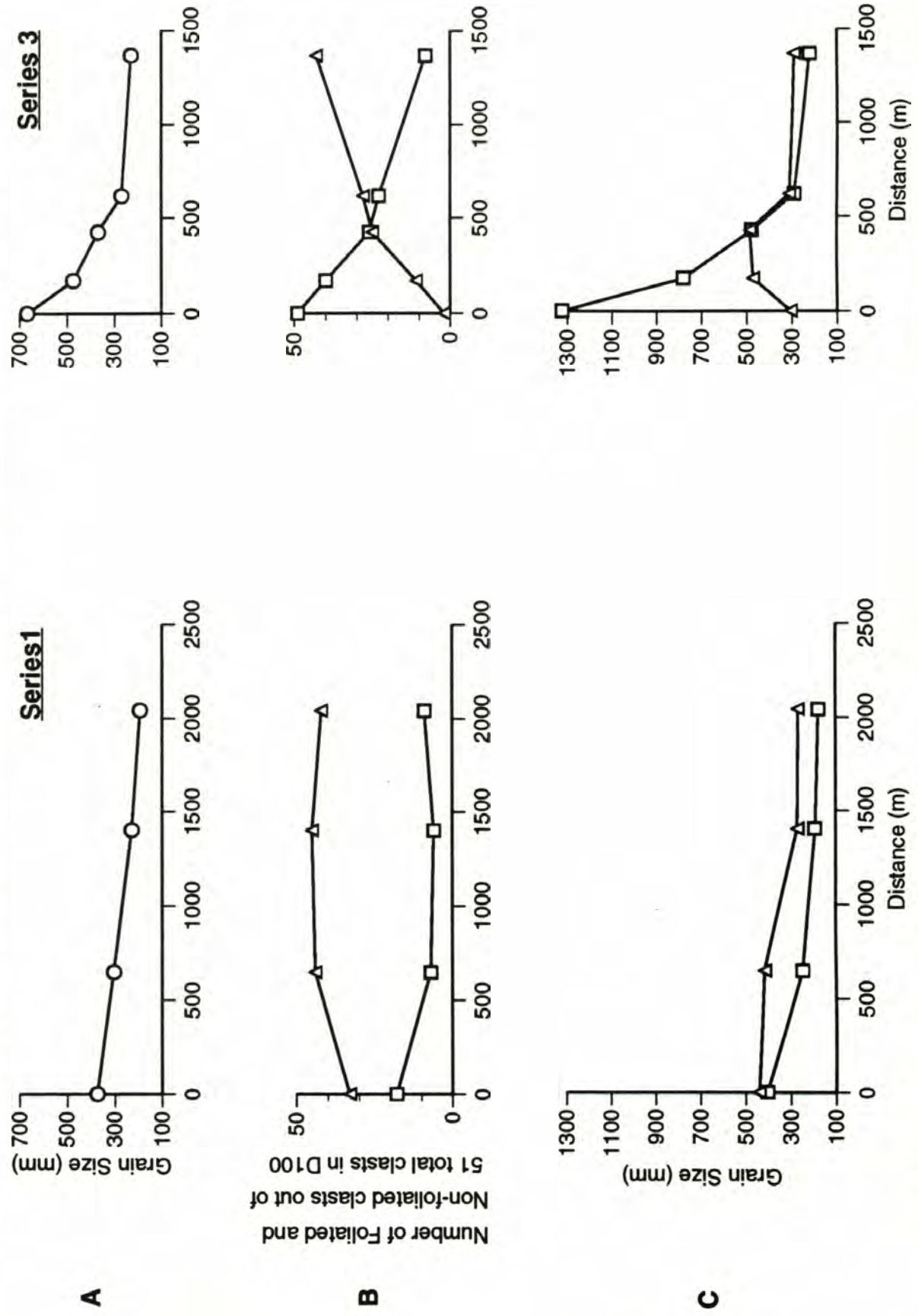


Figure 8



Table 5, and are shown graphically in Figure 8. Again, a fining trend is evident in the D100 data (Figure 8a), but this time using just fully exposed particles.

The two clast types do not exhibit the same rate of downstream fining (Table 5 and Figure 8c). Using the 12 largest clasts (fully exposed clasts) for each rock type, the overall fining trend is controlled most by the fining trend evident in the foliated particles. The particularly poor fit for the 12 largest non-foliated clasts of Series 3 can be attributed to mid-reach deposition of large particles from a slump along the channel bank, which originated in glacial fill material. The slump occurred between the second and third sample sites (Figure 2), below the phyllite bedrock gorge in which Series 3 originates.

The relative abundance of clasts of different lithology shows no consistent pattern for the two fining series (Figure 8b). For Series 1, the number of foliated particles and the number of non-foliated particles remain nearly constant through the 2-km reach over which fining occurs. For series 3, the number of foliated particles decreases and the number of non-foliated particles increases through the 1.5-km reach over which fining occurs.

## **CHANGES IN PARTICLE SHAPE WITH FINING**

In order to determine whether particle shapes changed with reduction in particle size, sphericity and form were determined for foliated and non-foliated rock types at the first and last sample sites in each of fining Series 1 and Series 3. The three orthogonal axes were measured on the 12 largest exposed particles of each lithology at a site, and axial measurements were converted into appropriate ratios.

### Sphericity versus Fining

At the beginning and end of Series 1 and Series 3, average maximum projection sphericity was calculated for the two classes of particles (foliated and non-foliated) based on each particle's sphericity derived from triaxial measurements (Table 6). Average sphericity is higher for the non-foliated class; sphericities range from 0.64 to 0.70 for non-foliated rock-types, and from 0.54 to 0.60 for the foliated rock-types (Table 6). Both average sphericity and the distribution of sphericities of both rock types did not appreciably change with fining in either Series 1 or Series 3 (Table 6). Average sphericity declined slightly for the foliated class of particles in Series 1.

### Changes in Clast Form versus Fining

Average form of the clasts in each rock type show generally consistent groupings in the two fining series. Non-foliated rock types are grouped between compact-bladed and bladed, and foliated rock type forms range between bladed and platy (Figure 9).

Changes in form between the first and last sample site are shown by arrows that link the initial shape to the final shape in each Series. In Series 1 foliated particle forms initially are bladed and become platy downstream, but in



TABLE 6: Data on Particle Shapes From the First and Last Sample Locations of Series 1 and Series 3

| <b>Foliated</b> |            |                     |             |                            |      |     |                      |      |               |                           |      |          |  |
|-----------------|------------|---------------------|-------------|----------------------------|------|-----|----------------------|------|---------------|---------------------------|------|----------|--|
| Fining Series   | Sample No. | Sample Distance (m) | Sample Size | Average axial lengths (mm) |      |     | Average axial ratios |      |               | Average sphericity $\Psi$ |      |          |  |
|                 |            |                     |             | a                          | b    | c   | c/a                  | mean | $(a-b)/(a-c)$ | mean                      | mean | $\sigma$ |  |
| Series 1        | 1          | 0                   | 12          | 666                        | 405  | 243 | 0.38                 | 0.10 | 0.55          | 0.26                      | 0.60 | 0.11     |  |
|                 | 2          | 2044                | 12          | 223                        | 177  | 85  | 0.38                 | 0.11 | 0.32          | 0.23                      | 0.56 | 0.12     |  |
| Series 3        | 1          | 0                   | 12          | 1835                       | 1325 | 623 | 0.35                 | 0.09 | 0.35          | 0.26                      | 0.54 | 0.09     |  |
|                 | 2          | 1370                | 12          | 320                        | 223  | 117 | 0.36                 | 0.13 | 0.44          | 0.24                      | 0.56 | 0.14     |  |

| <b>Non-foliated</b> |            |                     |             |                            |     |     |                      |      |               |                           |      |          |  |
|---------------------|------------|---------------------|-------------|----------------------------|-----|-----|----------------------|------|---------------|---------------------------|------|----------|--|
| Fining Series       | Sample No. | Sample Distance (m) | Sample Size | Average axial lengths (mm) |     |     | Average axial ratios |      |               | Average sphericity $\Psi$ |      |          |  |
|                     |            |                     |             | a                          | b   | c   | c/a                  | mean | $(a-b)/(a-c)$ | mean                      | mean | $\sigma$ |  |
| Series 1            | 1          | 0                   | 12          | 558                        | 442 | 255 | 0.46                 | 0.12 | 0.38          | 0.21                      | 0.64 | 0.11     |  |
|                     | 2          | 2044                | 12          | 355                        | 267 | 170 | 0.49                 | 0.13 | 0.44          | 0.23                      | 0.67 | 0.10     |  |
| Series 3            | 1          | 0                   | 12          | 409                        | 307 | 208 | 0.51                 | 0.10 | 0.48          | 0.19                      | 0.70 | 0.08     |  |
|                     | 2          | 1370                | 12          | 409                        | 292 | 198 | 0.50                 | 0.12 | 0.47          | 0.26                      | 0.69 | 0.08     |  |

Figure 9. Shapes of foliated and non-foliated particles of fining Series 1 and Series 3, plotted on the sphericity-form diagram of Sneed and Folk (1958) (Figure 4). The ternary diagrams are simplified to depict only the ratios used to calculate mean form. Open symbols designate foliated particles, closed symbols designate non-foliated particles.



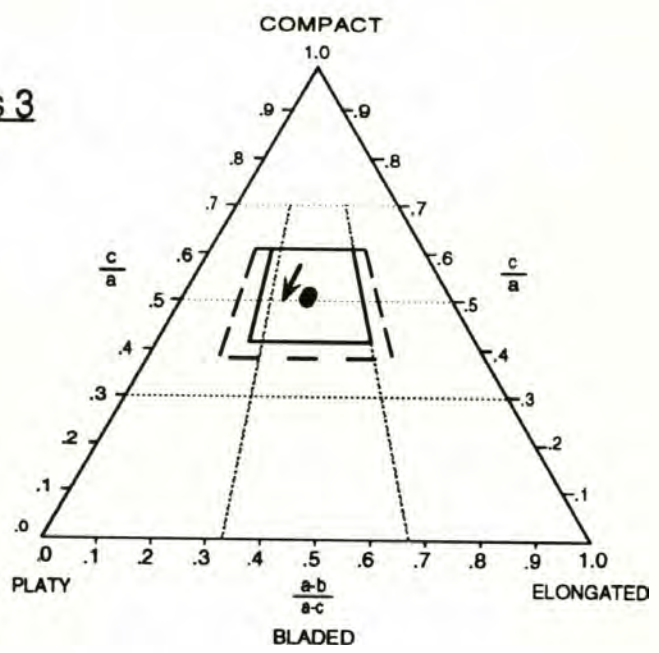
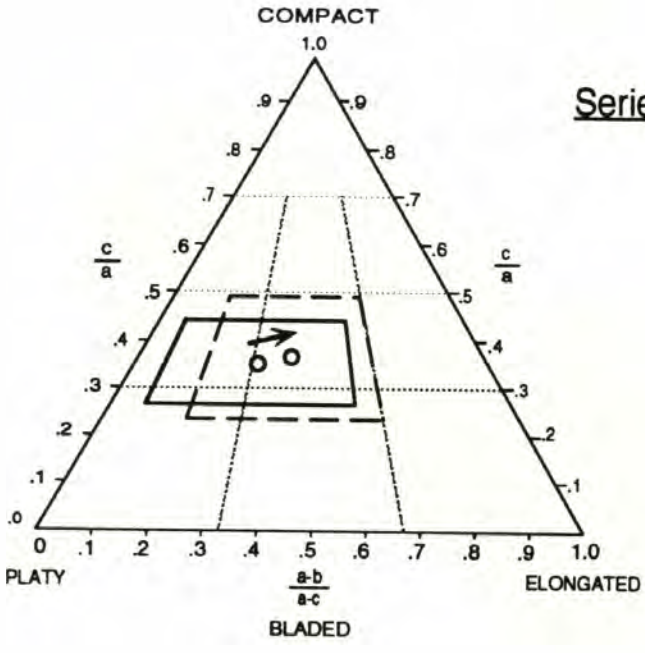
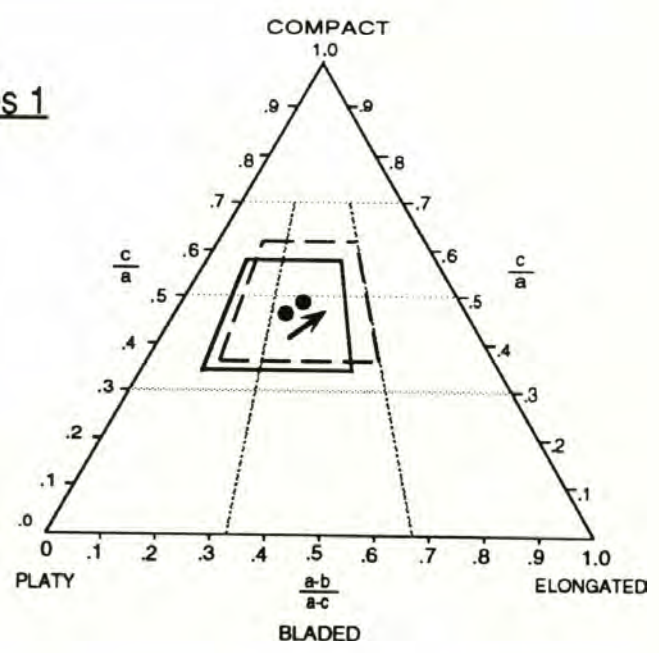
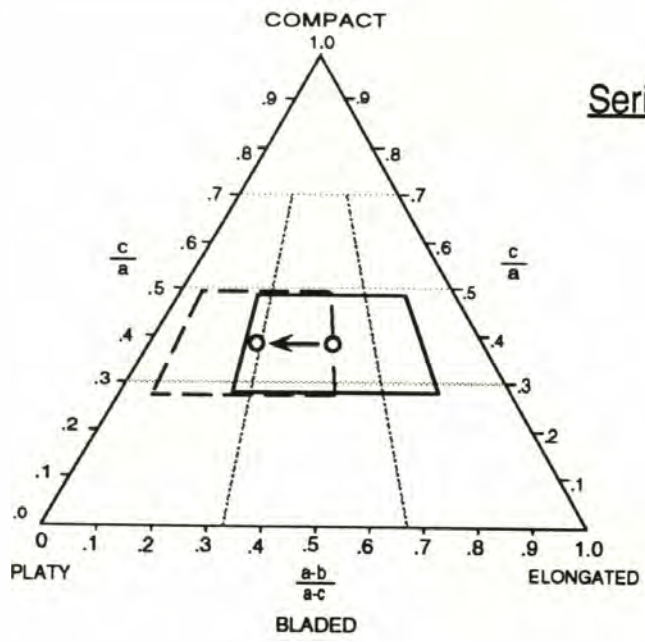
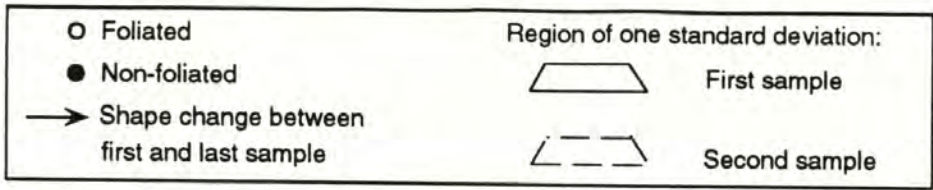


Figure 9

Series 3 the particle forms move from the region of platy to become bladed downstream (Figure 9). Non-foliated particle forms in Series 1 are bladed and change toward compact-bladed; but in Series 3, the change is in the direction away from compact-bladed toward bladed (Figure 9). Except for the foliated clast forms in Series 1, changes of average form appear to be small compared to the range of measures at the beginning and end of the respective fining series (Table 6; Figure 9).



## **ABRASION TANK STUDY**

An experiment of mechanical abrasion was performed to determine the relative rates of change in size and shape caused by abrasion for the foliated and non-foliated rock types. Seven pairs of Finney Creek particles were transported a total distance of five kilometers each in a circulating flume (see Appendix I for a description of the flume). Each pair consisted of one large foliated and one large non-foliated clast; sizes ranged between 175 and 232 mm (intermediate axis). All samples used in the study were collected from the first fining reach (Series 1). The principal axes (a, b and c) were measured, and the dry mass was recorded for each rock before transport in the flume. The pairs were transported with about 35 kg of coarse sand and fine gravel over a hard bed of cobbles embedded in cement. The particles were transported for 2.5 km, their axes were measured again, and then the particles were transported another 2.5 km. A final measure was taken of the axes and the dry mass. Average water depth was 0.28 m, mean water velocity was  $2.8 \text{ m sec}^{-1}$ , and mean particle velocity ranged from  $0.57$  to  $0.81 \text{ m sec}^{-1}$  for the seven pairs.

Results are summarized in Table 7 and Figure 10. Mean size reduction (intermediate axis) for each rock type was greater in the first 2.5 km of transport than in the second (bottom, Table 7). In the first run of 2.5 km the greatest reduction of axial lengths for both rock types occurred on the intermediate and short axes (b-axis and c-axis, Table 7). In contrast, foliated particle's average of axial reductions during the second run indicates that the greatest wear was on the long axis. However, this is due to a single particle, foliated sample number 6, which broke apart during transport. If axial reductions from this particle are excluded from the average of axial reductions during the second run, then the results are similar to the first run; the greatest wear occurred on the intermediate



TABLE 7: Abrasion Tank Data On Size And Shape

| Sample Rock no.*<br>Type† | b-axis (mm) |        | a-axis<br>Reduction<br>(mm) | c-axis<br>Reduction<br>(mm) | c/a   |        | (a-b)/(a-c) |       | Sphericity $\Psi$ |         | Mass (kg) |        |         |       |        |        |        |        |      |
|---------------------------|-------------|--------|-----------------------------|-----------------------------|-------|--------|-------------|-------|-------------------|---------|-----------|--------|---------|-------|--------|--------|--------|--------|------|
|                           | Start       | Finish |                             |                             | Start | Finish | Change§     | Start | Finish            | Change§ | Start     | Finish | Change§ | Start | Finish |        |        |        |      |
| 1a                        | 194         | 161    | 33                          | 6                           | 0.39  | 0.43   | 0.39        | 0.54  | 0.68              | 0.71    | 0.14      | 0.64   | 0.64    | 0.00  | 6.660  | 5.020  | 1.64   |        |      |
| 1b                        | 161         | 153    | 8                           | 11                          | 0.39  | 0.40   | 0.40        | 0.68  | 0.71              | 0.03    | 0.64      | 0.66   | 0.66    | 0.02  | 0.01   | 10.625 | 9.210  | 1.42   |      |
| 2a                        | 213         | 203    | 10                          | 14                          | 0.51  | 0.52   | 0.52        | 0.47  | 0.57              | 0.01    | 0.70      | 0.71   | 0.71    | 0.00  | 0.03   | 10.700 | 6.760  | 3.94   |      |
| 2b                        | 203         | 187    | 16                          | 1                           | 0.52  | 0.51   | 0.51        | 0.47  | 0.57              | -0.02   | 0.47      | 0.71   | 0.71    | 0.00  | -0.04  | 0.00   | 3.360  | 5.13   |      |
| 3a                        | 221         | 191    | 30                          | 16                          | 0.54  | 0.48   | 0.48        | 0.43  | 0.51              | -0.06   | 0.43      | 0.68   | 0.68    | -0.03 | -0.17  | 8.490  | 6.760  | 3.94   |      |
| 3b                        | 191         | 175    | 16                          | 3                           | 0.48  | 0.42   | 0.42        | 0.51  | 0.55              | 0.04    | 0.68      | 0.64   | 0.64    | 0.04  | 0.04   | 10.545 | 8.535  | 2.01   |      |
| 4a                        | 213         | 186    | 27                          | 5                           | 0.60  | 0.38   | 0.38        | 0.31  | 0.35              | -0.22   | 0.31      | 0.74   | 0.57    | 0.04  | 0.04   | 10.330 | 1.670  | 8.66   |      |
| 4b                        | 186         | 179    | 7                           | 16                          | 0.38  | 0.27   | 0.27        | 0.35  | 0.27              | -0.11   | 0.35      | 0.45   | 0.45    | -0.09 | -0.12  | 0.00   | 7.460  | 3.02   |      |
| 5a                        | 179         | 172    | 7                           | 5                           | 0.49  | 0.47   | 0.47        | 0.72  | 0.71              | -0.02   | 0.72      | 0.71   | 0.71    | 0.00  | -0.01  | 10.545 | 8.535  | 2.01   |      |
| 5b                        | 172         | 168    | 4                           | 6                           | 0.47  | 0.46   | 0.46        | 0.71  | 0.71              | 0.00    | 0.71      | 0.70   | 0.70    | 0.00  | 0.00   | 10.330 | 1.670  | 8.66   |      |
| 6a                        | 220         | 182    | 38                          | 21                          | 0.49  | 0.41   | 0.41        | 0.50  | 0.58              | -0.08   | 0.50      | 0.69   | 0.64    | -0.05 | -0.05  | 10.330 | 1.670  | 8.66   |      |
| 6b                        | 182         | 117    | 65                          | 117                         | 0.41  | 0.46   | 0.46        | 0.58  | 0.48              | 0.04    | 0.58      | 0.65   | 0.65    | -0.10 | -0.10  | 0.00   | 7.460  | 3.02   |      |
| 7a                        | 208         | 171    | 37                          | 27                          | 0.55  | 0.50   | 0.50        | 0.63  | 0.71              | -0.05   | 0.63      | 0.75   | 0.73    | 0.08  | 0.08   | 10.480 | 7.460  | 3.02   |      |
| 7b                        | 171         | 164    | 7                           | 4                           | 0.50  | 0.46   | 0.46        | 0.71  | 0.69              | -0.04   | 0.71      | 0.70   | 0.70    | -0.02 | -0.04  | 0.00   | 9.250  | 8.10   | 0.44 |
| 8a                        | 195         | 192    | 3                           | 0                           | 0.49  | 0.48   | 0.48        | 0.49  | 0.51              | 0.00    | 0.49      | 0.68   | 0.68    | 0.02  | 0.02   | 0.00   | 8.350  | 8.200  | 0.15 |
| 8b                        | 192         | 190    | 2                           | 0                           | 0.48  | 0.48   | 0.48        | 0.51  | 0.51              | -0.01   | 0.51      | 0.68   | 0.68    | 0.01  | 0.01   | 0.00   | 12.625 | 12.410 | 0.22 |
| 9a                        | 178         | 176    | 2                           | 0                           | 0.52  | 0.52   | 0.52        | 0.59  | 0.60              | -0.01   | 0.59      | 0.73   | 0.72    | 0.01  | 0.01   | 0.00   | 9.685  | 9.330  | 0.35 |
| 9b                        | 176         | 174    | 2                           | 1                           | 0.52  | 0.51   | 0.51        | 0.60  | 0.61              | 0.00    | 0.60      | 0.73   | 0.73    | 0.01  | 0.01   | 0.00   | 10.515 | 10.010 | 0.51 |
| 10a                       | 217         | 217    | 0                           | 0                           | 0.56  | 0.56   | 0.56        | 0.45  | 0.45              | 0.00    | 0.45      | 0.73   | 0.73    | 0.00  | 0.00   | 0.00   | 10.095 | 9.560  | 0.53 |
| 10b                       | 217         | 217    | 0                           | 1                           | 0.56  | 0.56   | 0.56        | 0.45  | 0.45              | 0.00    | 0.45      | 0.73   | 0.73    | 0.00  | 0.00   | 0.00   | 11.685 | 10.280 | 1.41 |
| 11a                       | 190         | 186    | 4                           | 0                           | 0.53  | 0.52   | 0.52        | 0.59  | 0.61              | -0.01   | 0.59      | 0.73   | 0.73    | 0.02  | 0.02   | 0.00   | 10.010 | 10.010 | 0.51 |
| 11b                       | 186         | 183    | 3                           | 0                           | 0.52  | 0.52   | 0.52        | 0.61  | 0.63              | 0.00    | 0.61      | 0.73   | 0.73    | 0.02  | 0.02   | 0.00   | 10.095 | 9.560  | 0.53 |
| 12a                       | 175         | 174    | 1                           | 3                           | 0.62  | 0.61   | 0.61        | 0.84  | 0.81              | -0.01   | 0.84      | 0.82   | 0.82    | -0.03 | -0.03  | 0.00   | 11.685 | 10.280 | 1.41 |
| 12b                       | 174         | 174    | 0                           | 2                           | 0.61  | 0.61   | 0.61        | 0.81  | 0.81              | 0.00    | 0.81      | 0.82   | 0.82    | 0.00  | 0.00   | 0.00   | 10.010 | 10.010 | 0.51 |
| 13a                       | 197         | 195    | 2                           | 2                           | 0.63  | 0.63   | 0.63        | 0.53  | 0.53              | 0.00    | 0.53      | 0.79   | 0.79    | 0.00  | 0.00   | 0.00   | 10.095 | 9.560  | 0.53 |
| 13b                       | 195         | 194    | 1                           | 2                           | 0.63  | 0.63   | 0.63        | 0.53  | 0.52              | 0.00    | 0.53      | 0.79   | 0.79    | -0.01 | -0.01  | 0.00   | 11.685 | 10.280 | 1.41 |
| 14a                       | 232         | 226    | 6                           | 2                           | 0.59  | 0.56   | 0.56        | 0.47  | 0.48              | -0.03   | 0.47      | 0.74   | 0.74    | 0.01  | 0.01   | 0.00   | 10.010 | 10.010 | 0.51 |
| 14b                       | 226         | 221    | 5                           | 3                           | 0.56  | 0.55   | 0.55        | 0.48  | 0.49              | -0.01   | 0.48      | 0.74   | 0.73    | -0.01 | -0.01  | 0.00   | 9.800  | 9.800  | 0.52 |

| Averages | 207 | 181 | 26 | 13 | 23 | 0.51 | 0.45 | -0.06 | 0.51 | 0.57 | 0.06  | 0.71 | 0.67 | -0.04 | 9.690  | 6.002 | 3.69 |
|----------|-----|-----|----|----|----|------|------|-------|------|------|-------|------|------|-------|--------|-------|------|
| a        | 181 | 163 | 18 | 23 | 16 | 0.45 | 0.43 | -0.03 | 0.57 | 0.57 | -0.01 | 0.67 | 0.64 | -0.02 | 0.00   | 6.002 | 3.69 |
| b        | 198 | 195 | 3  | 1  | 2  | 0.56 | 0.55 | -0.01 | 0.57 | 0.57 | 0.00  | 0.75 | 0.74 | -0.01 | 10.315 | 9.800 | 0.52 |
| a        | 195 | 193 | 2  | 1  | 2  | 0.55 | 0.55 | 0.00  | 0.57 | 0.57 | 0.00  | 0.74 | 0.74 | 0.00  | 9.800  | 9.800 | 0.52 |

\* Data reported in row "a" of each numbered sample is from the first run of about 2500 m of particle transport. Data reported in row "b" is from the second run of the same sample. The total distance of transport from both runs is about 5000 m for each sample.

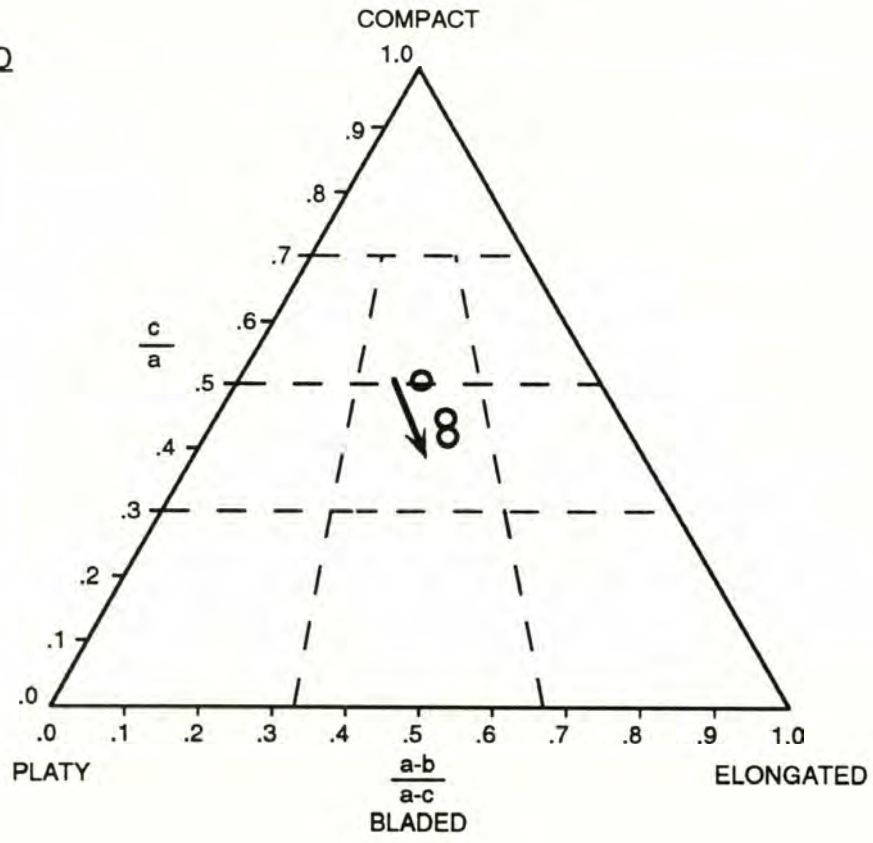
† F = foliated, NF = non-foliated

§ Change = the difference between the finish and start ratios. Some reported differences show discrepancies due to rounding in the calculations.



Figure 10. Form diagrams showing changes in particle form in the abrasion tank experiment. Open symbols designate foliated particles, closed symbols designate non-foliated particles. For non-foliated particles, three data points are plotted but the second and third shape measurements (lower closed circle) are the same.

FOLIATED



NON-FOLIATED

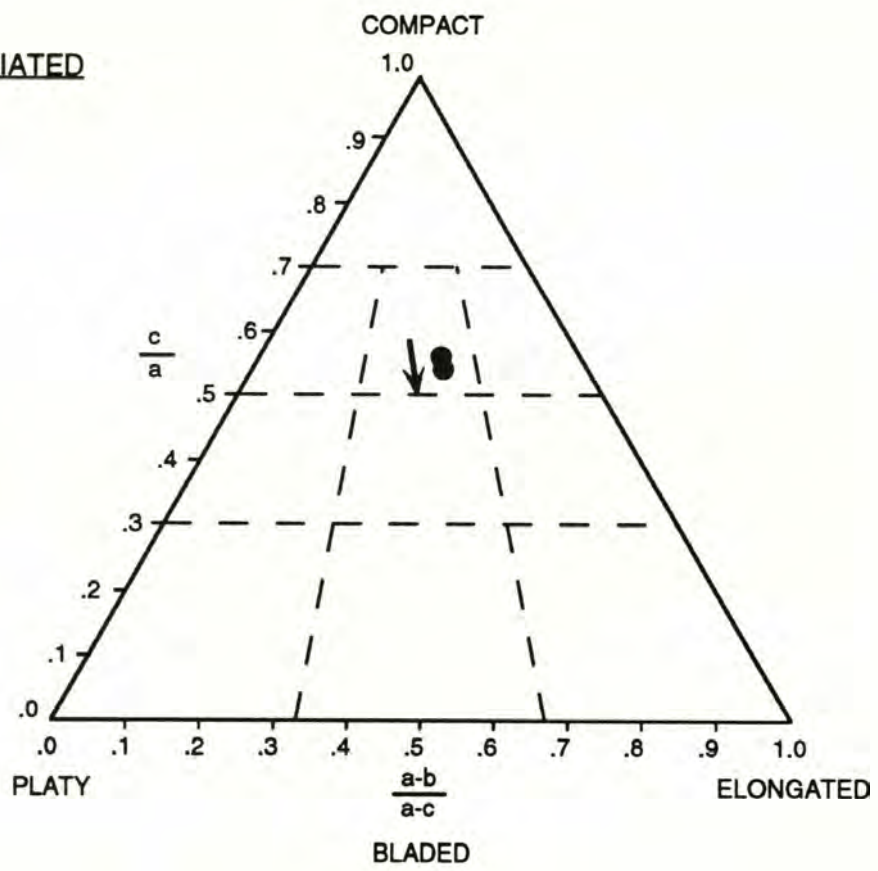


Figure 10



and short axes. The greater wear on the intermediate and short axes suggests that particles moved by rolling rather than by sliding or tumbling end over end.

Form and sphericity changes were greater for the foliated particles; non-foliated specimens changed very little (Figure 10; Table 7). For the foliated specimens, average form changed rapidly in the first 2.5 km of transport and more slowly in the final 2.5 km of transport (Figure 10). Average form of the foliated particles changed from compact-bladed to bladed.

## DISCUSSION

Downstream particle fining in the Finney Creek channel is evident over short distances for the coarsest fraction of particles, and the fining trends are spatially associated with recent deposition of coarse clasts from debris slides and debris flows. For the field data, analysis of fining trends by lithologic differences between the principle rock types and by particle shape does not provide sufficient constraints to assess the relative importance of selective transport versus abrasion as fining mechanisms for particles smaller than 400 mm. Sediment supplied from multiple sources along channel, combined with the short distances over which fining occurs, are the principle deterrents to a definitive field evaluation of fining mechanisms. However, by combining field and abrasion tank data, and using assumptions about the correlation of these two data sets, qualified conclusions can be made about the influence of clast lithology and clast size on fining mechanisms.

### Fining Trends and Coarse Sediment Input from Debris Flows and Debris Slides

Four particle-fining trends are evident in the upper half of the study reach, where particle fining is spatially related to recent (2 - 14 year) channel deposits from debris flows and debris slides (Figure 5). Fining trends are not evident in the lower half of the study reach (Figure 5); three debris flow deposits in the lower portion of the study reach did not correlate with reductions in particle size. The apparent absence of particle fining in the lower reach can be related in part to the valley geometry. The lowermost Finney Creek valley, which includes the lower reaches of the downstream-most tributaries, is part of a broad valley that is graded to the Skagit River. The largest clasts from debris flows deposited in the downstream-most tributaries never make it to Finney Creek.



The four fining trends in the upper portion of the study reach are best exhibited by the coarsest particles in the channel. Particle sizes decrease rapidly downstream from the source deposit, the largest size changes occurring in the first 1000 m of the deposit. If one were to ignore the size data from sample sites in the first 1000 m of each fining series, then the distribution of the D100 in the upstream half of a sample reach would lack a distinctive fining trend and thus be similar in this sense to the distribution of the D100 in the lower half of the sample reach (Figure 5).

Based on Finney Creek field data, particles larger than 400 mm are inferred to move infrequently relative to particles smaller than 400 mm. This upper-size limit is derived from two observations; first, this size exceeds the upper limit of the D100 in the lower half of the study reach, and second, this size exceeds the D100 sizes found at the tails of the fining trends in the upper reach. It thus appears that 400 mm approximates an upper boundary for the largest-sized particles that Finney Creek is competent to transport within the study reach .

Particles larger than 400 mm are generally immobile, abrade in place and tend to become buried. For example, in the first two sample sites of Series 3, quartz veins in some large foliated particles project by several centimeters from the phyllite where the phyllite has been preferentially worn away due to abrasion in place. These larger particles are partially buried by more mobile smaller particles. Figure 11 compares particle fining trends of the D100 that includes partially buried particles (Figure 6) with fining trends of the D100 that includes only fully exposed particles (Figure 8a). Fining trends of both data sets are essentially equivalent for sizes that are 400 mm and smaller.

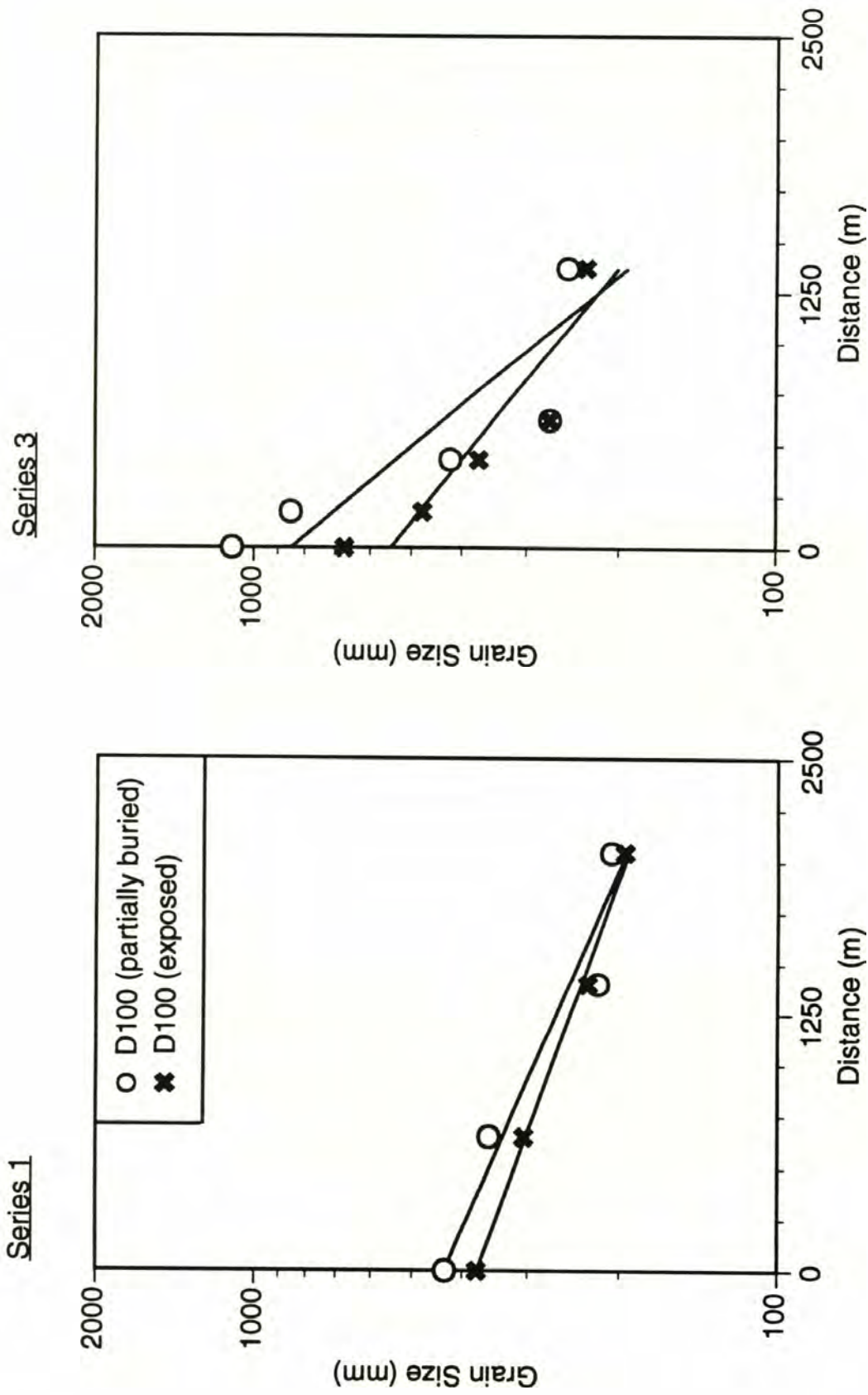


Figure 11. Comparison of particle fining trends for partially buried (open circles) and fully exposed (crosses) particles of the D100 in fining Series 1 and 3.



### Insights Into Fining Mechanisms for Particles Less Than 400 mm: Field Data

Because particles larger than 400 mm are relatively immobile and are subject to burial by particles that the stream is competent to move, then size sorting by selective transport is clearly an important process for these particles. Transport of the largest particles in Finney Creek must be selective because the stream does not have the capacity to transport all the sediment delivered to it. However, D100-sized particles less than 400 mm do not fine only by selective transport; abrasion tank data indicate that some of the fining is attributable to abrasion of the particles as they move along the bed of the stream.

Evaluating the proportion of fining attributable to abrasion for particles less than 400 mm was attempted in field and experimental investigations. In the field, observed fining trends were analyzed by lithology of the principle rock types of the D100. Unfortunately, as mentioned previously, this analysis is complicated by bank erosion of Quaternary glacial sediment that provides the non-foliated particles along the stream reaches with the observed fining trends. The abundance of D100 foliated particles declines from the sites of initial deposition in some reaches (Figure 7 lower, and Figure 8b). Based on a decline in abundance of foliated particles as a percentage of the D100, I infer preferential attrition of the foliated particles for that size class. However, the decreasing relative abundance of foliated clasts with fining may be due in part to an increase in the number of non-foliated clasts due to bank erosion.

Downstream decreases of particle size are generally greater for the foliated class of particles (Figure 8 and Table 5). In Series 1, the initial average sizes of foliated and non-foliated particles are nearly equal; thereafter, sizes of foliated particles are less than the non-foliated sizes (Figure 8c). However, the rates of fining (fining coefficients in Table 5) do not differ appreciably between the rock



types over the length of the reach in Series 1. In Series 3 the fining rates differ by an order of magnitude (Table 5) over the length of the reach, but initial sizes of the lithologies are not related; all non-foliated particles in Series 3 were not supplied from a single source at the head of the fining series. However, from the third sample site to the last, size reductions proceed at about the same rate (Figure 8c). The third sample site is located where coarse non-foliated particles are contributed from a bank-side slump. In both fining series, size reduction appears to proceed at about the same rate for both lithologies despite complications to the relative abundance of lithologies caused by introduction of new material from channel bank failures.

#### Particle Shape Changes with Downstream Changes in Particle Size: Field versus Tank Data

Average sphericities of both foliated and non-foliated rock types fall within a narrow range, and the sphericities do not change appreciably with fining (Table 6). Though the foliated particles do not become more spherical, they do tend to become either more platy or bladed while retaining roughly the same  $c/a$  ratio (Figure 9).

Foliated and non-foliated particles at the first sample site in Series 1 are nearly equal in size (Figure 8c), including volume and mass (average volumes of both rock types are between  $3.3 \times 10^7$  and  $3.4 \times 10^7$  mm<sup>3</sup>), and their forms are bladed (Figure 9). However, below the first sample location, sizes of the non-foliated class of particles are everywhere larger than sizes of the foliated class of particles. Also, the change of form downstream for non-foliated particles shows a tendency toward compact, and sphericity of such particles increases.

These observations from the field suggest two alternative interpretations. The first interpretation is that smaller platy foliated particles are preferentially



transported from their upstream source along with larger, more compact non-foliated particles. This alternative would require flows sufficient to overcome the resistance to tractive transport offered by the platy particle forms.

The second interpretation is that the shapes of the foliated particles are produced by wear during transport, and therefore the shape changes are the product of abrasion rather than selective downstream transport. In this second interpretation, the more spherical particles of both rock types are winnowed from upstream. However, particle wear during transport then proceeds more rapidly for foliated particles than for non-foliated particles.

The abrasion tank data support the second alternative but not the first. The tank data show that foliated particles abrade much more than non-foliated particles; total mass lost due to abrasion of the foliated particles was about 7 times greater than for the non-foliated particles (Table 7). In addition, observations from the abrasion tank study indicate that particle shapes do affect mobility. Of non-foliated and foliated particles of equal mass that duplicated the range of form and sphericity of particles from the first sample site in Series 1, platy foliated particles did not move at all in the tank under flow conditions that transported non-foliated and foliated compact-bladed particles with higher sphericities. Hence, foliated particles that had a compact-bladed form were chosen for transport in the tank.

#### Combining Tank and Field Data: Approximating the Separate Contributions of Abrasion and Sorting Processes to Fining Mechanisms

The reduction of grain size can be described exponentially in the four fining reaches of Finney Creek. An exponential decrease of particle size downstream is described by the equation whose general form is  $y=be^{-ax}$  in which



$y$  is the particle size at some distance  $x$  downstream of where the initial particle size  $b$  is measured, and the constant  $a$  is the coefficient of fining.

The equation  $y=be^{-ax}$  can be expanded to  $y=be^{-(a_1 + a_2)x}$  in which  $a_1$  is the coefficient of abrasion and  $a_2$  is the coefficient of sorting by selective transport (Knighton, 1980). Most empirical studies calculate a single coefficient and the separate effects of sorting and abrasion remain hidden. I will make the case that results obtained from my abrasion tank studies can be used, in conjunction with the field results, to estimate a range of the separate rates of size reduction due to abrasion and selective transport for foliated and non-foliated particles in the Series 1 fining reach of Finney Creek.

Results from the abrasion experiment show that in five km of transport the reduction of size ( $b$ -axis) due to abrasion is about nine times greater for foliated particles than for non-foliated particles (Table 7). For the sake of comparison to field data on fining, exponential equations are fitted to the tank-determined grain size reduction data (Figure 12). The coefficient of abrasion ( $a_1$ ) of the foliated particles is 0.05, an order of magnitude greater than that of the non-foliated particles, which is 0.005 (Figure 12).

Coefficients of abrasion for the field data would be at least as large as the coefficients derived from the tank data because tank-derived abrasion coefficients are minimums. Tank-derived abrasion coefficients are minimums because many transits around a circular flume are required to represent the in-place motion and abrasion of coarse particles on a river bed (Schumm and Stevens, 1973). Hence, results obtained from abrasion experiments may underestimate by as much as 10 times the actual amount of abrasion that occurs over an equivalent distance in the stream channel (Schumm and Stevens, 1973). However, the tank-derived abrasion coefficients are none-the-less illuminating as to the relative importance of abrasion for the two clast lithology types. Both the



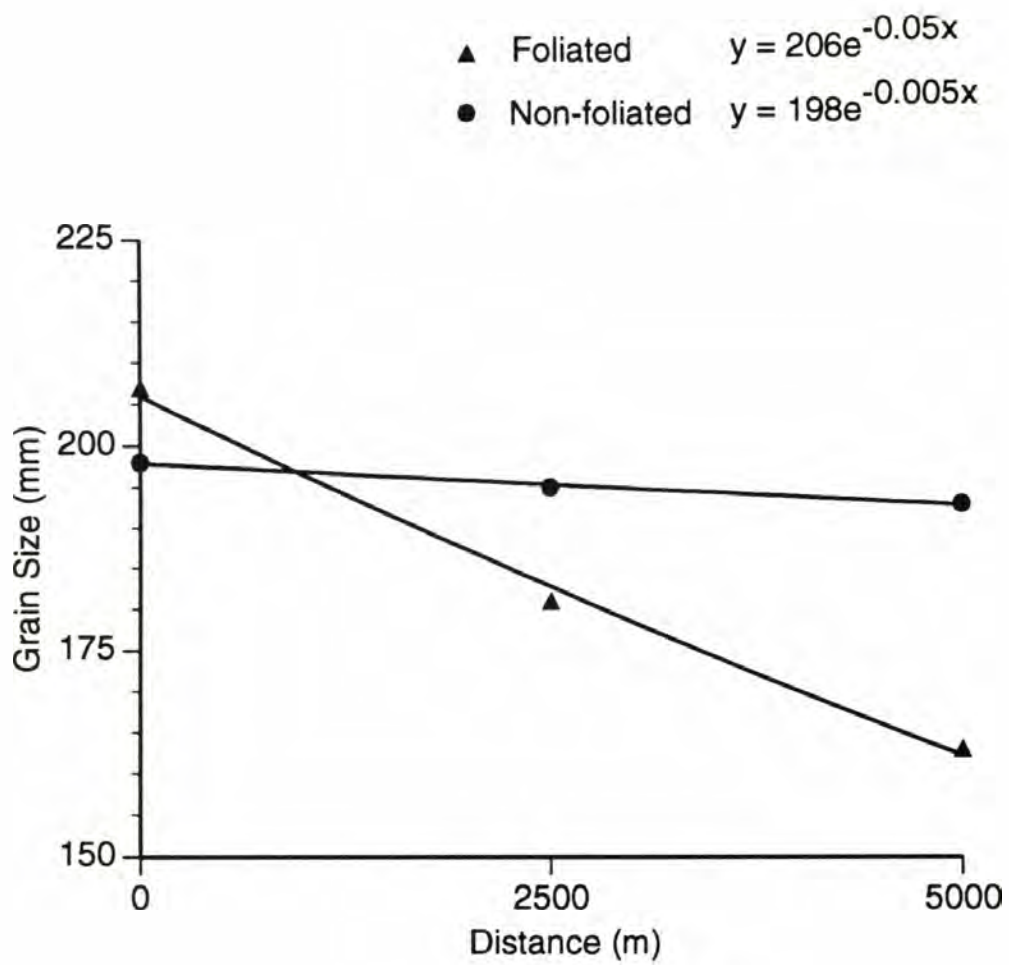


Figure 12. Plot of grain sizes (b-axis) of foliated and non-foliated particles transported in the abrasion experiment, and the exponential curves that describe the reduction of grain size.

Figure 13. Plots of predicted D100 grain size versus distance for foliated and non-foliated particles in Series 1. Curves are plots of exponential equations derived from combined field and experimental data. Curve  $y_F$  is the best-fit relation from the field data. Curve  $y_T$  utilizes experimental results to predict grain size as a function of abrasion.  $a_1$  is the coefficient of fining due to abrasion.  $a_2$  is the coefficient of fining due to selective transport. Coefficient  $b$  is observed.



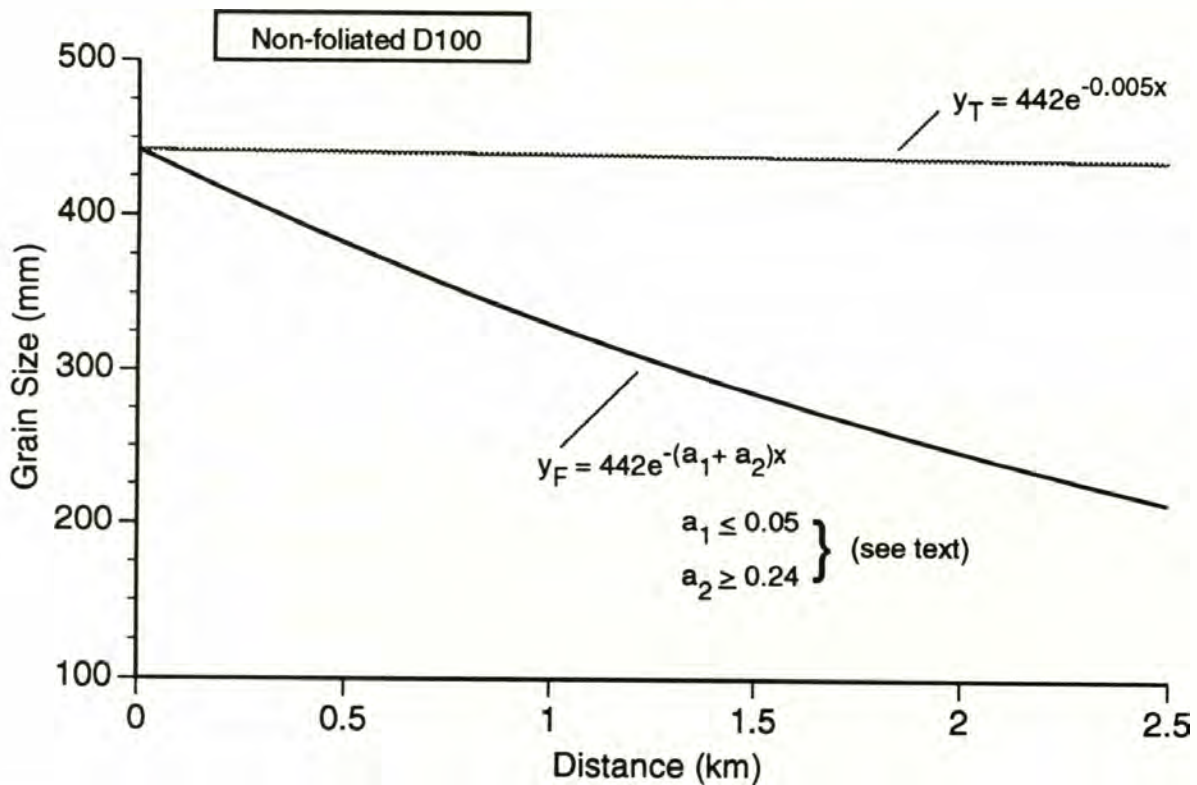
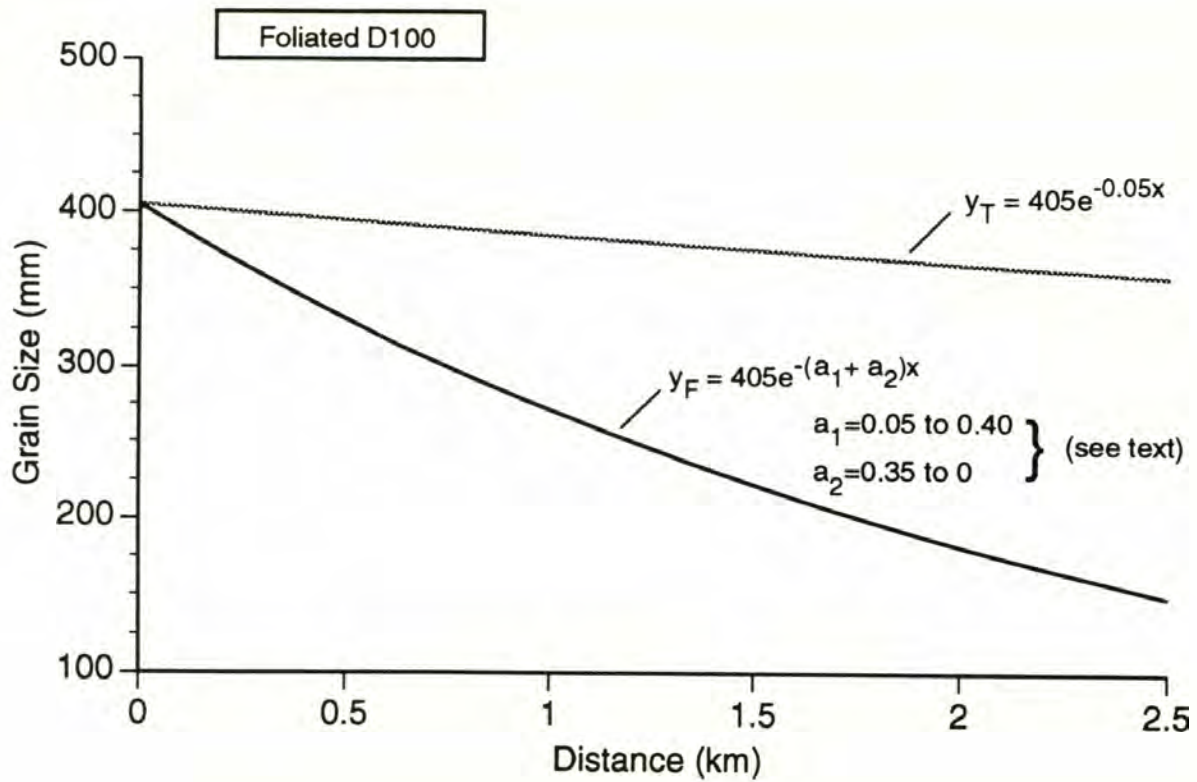


Figure 13

abrasion experiment and field observations indicate that the effects of abrasion on the reduction of grain size of the non-foliated particles are minor; non-foliated particles showed only small percussion marks and very little evidence of cracking, splitting, or chipping. Conversely, all evidence discussed above shows that abrasional processes are relatively important in reducing the sizes of the foliated particles.

An upper boundary on the range of values of the coefficient of abrasion for the foliated particles is limited only by the overall coefficient of fining, which is 0.40. Neither field relations nor observations from the abrasion experiment are sufficient to estimate the proportion of fining by abrasion on the total reduction of sizes of the foliated particles, except that abrasion may account for 100% of total reduction. Thus, estimates of the coefficients of abrasion for particles in Series 1 of Finney Creek range between 0.05 and 0.40 for foliated particles (Figure 13).

In contrast, non-foliated particles transported in the channel and in the tank suffer very little reduction in size from abrasion; very few non-foliated particles in the channel were broken, chipped or cracked, and non-foliated particles transported in the tank showed only percussion marks from impacts. Shapes of non-foliated clasts are inherited from previous erosion processes, and these shapes do not change appreciably downstream (Table 6, Figure 9). Thus, the tank-derived coefficient of fining due to abrasion for the non-foliated particles is small. Even if I assume it is 10 times larger than that determined in the tank (0.005), it is still only about 17% of the total fining coefficient, the rest of which must be attributed to selective transport.

Experimental abrasion results applied to field relations, together with evidence that definitively shows selective transport of particles larger than 400 mm, indicate that selective transport is the dominant mechanism responsible for the observed fining trends for non-foliated rock types in the Finney Creek



channel. The components of fining that can be attributed to abrasion during transport over several kilometers of distance is greater than 10% and most likely approaches 100% for foliated particles less than 400 mm in size, and is less than 17% for non-foliated particles smaller than 400 mm in size.

## **SUMMARY**

The grain size distributions of coarse particles, and the distributions of coarse particle shapes and lithologies, were investigated in Finney Creek, a mountain stream channel in northwest Washington with an historically high incidence of sedimentation from landslides. The investigation showed that the size of the coarsest particles, defined by the median size of the 51 largest particles measured at a site, exhibits an orderly decline downstream from sources of coarse debris delivered to the channel. While fining trends appear to be influenced by shapes of the principle lithologies, durability of the principal rock types is a more important determinant of the fining mechanism.

Four distinct downstream trends of particle fining are spatially associated with recent deposition of coarse clasts in the channel from debris slides and debris flows. These trends of particle fining are evident over relatively short distances (1370 m to 2430 m). Particle sizes diminish rapidly downstream from the debris source, and in all trends approach a common minimum value. The distance over which fining occurs appears to be dictated in every fining series by the occurrence of a recent debris slide or debris flow deposit.

Fining trends for the two principal rock types in the channel are strongly related to their relative abundance. Analysis of fining trends by lithology of the principle rock types shows that overall trends are influenced most by the fining trend evident in the foliated rock type and least by the trend evident in the non-foliated rock type. This observation is attributed primarily to contamination from erosion of channel banks comprised of glacial fill material from which the non-foliated rock type is derived.

Longitudinal changes in the lithologic composition of the coarsest clasts suggest that selective transport occurs for all particles of size greater than about 400 mm, but below that size the primary fining mechanism is different for the two



rock types. Experimental results from the abrasion tank study demonstrated that foliated particles abrade at about 10 times the rate of non-foliated particles. The best insight into the relative effects of abrasion versus selective transport comes from combining results of the field and tank data. Assessments of the correlation between tank and field data indicate that abrasion processes account for 10 to 100% of the total reduction of grain size of foliated clasts, and less than 17% of the total size reduction of non-foliated clasts.

## REFERENCES

- Benda, L., 1989, The influence of debris flows on channels and valley floors in the Oregon Coast Range, U.S.A., *Earth Surface Processes and Landforms*, 15, 457-466.
- Bradley, W.C., 1970, Effects of weathering on abrasion of gravel, Colorado and Texas, *Geological Society of America Bulletin*, 81, 61-80.
- Bradley, W.C., Fahnestock, R.K., and Rowekamp, E.T., 1972, Coarse sediment transport by flood flows on the Knik River, Alaska, *Geological Society of America Bulletin*, 83, 1261-1284.
- Brierly, G.J., and Hicken, E.J., 1985, The downstream gradation of particle size in the Squamish River, British Columbia, *Earth Surface Processes and Landforms* 10, 597-606.
- Brown, E.H., Blackwell, D.L., Christenson, B.W., Frasse, F.I., Haugarud, R.A., Jones, J.T., Leiggi, P.A., Morrison, M.L., Rady, P.M., Reller, G.J., Seivigny, C.B., 1987, *Geologic Map of the Northwest Cascades, Washington: Geological Society of America Map and Chart Series MC-61, scale 1:100000.*
- Church, M., and Kellerhals, R., 1978, On the statistics of grain size variation along a gravel river, *Canadian Journal of Earth Sciences*, 15, 1151-1160.
- Cummins, J.E., Collings, M.R., and Nassar, E.G., 1975, Magnitude and frequency of floods in Washington: U.S. Geological Survey Open-File Report 74-336, 46 p.
- Harr, R.D., Coffin, B.A., and Cundy, T.W., 1989, Effects of timber harvest on rain-on-snow run-off in the transient snow zone of the Washington Cascades, Interim final report submitted of TFW Sediment, Hydrology, and Mass Wasting Steering Committee (Washington state).
- Knighton, A.D., 1980, Longitudinal changes in size and sorting of stream-bed material in four English rivers, *Geological Society of America Bulletin*, 91, 55-62.
- Krumbein, W.C., 1941, The effects of abrasion on the size, shape and roundness of rock fragments, *Journal of Geology*, 49, 482-520.
- Krumbein, W.C., 1942, Settling-velocity and flume-behavior of non-spherical particles, *Trans. Am. Geophys. Union*, 621-633.



- Krumbein, W.C., and Graybill, F.A., 1965, An introduction to statistical models in geology, McGraw-Hill, Inc., New York, 475 p.
- Kuenen, P.H., 1956, Experimental abrasion of pebbles: 2. Rolling by current: *Jour. Geology*, v. 64, p. 336-368.
- National Climatic Data Center, 1991, Daily precipitation values for Concrete, Washington.
- Paola, C., Parker, G., Seal, R., Sinha, S.K., Southard, J.B., Wilcock, P.R., 1992, Downstream fining by selective deposition in a laboratory flume, *Science*, 258, 1757-1760.
- Parks, D.S., 1992, A landslide inventory of the Finney Creek watershed, Skagit County, Washington, M.S. Thesis, University of Washington, Seattle, Washington, 164 pp.
- Schumm, S.A., and Stevens, M.A., 1973, Abrasion in place: a mechanism for rounding and size reduction of coarse sediments in rivers, *Geology*, 1, 37-40.
- Shaw, J. and Kellerhals, R., 1982, The composition of recent alluvial gravels in Alberta river beds, *Bulletin of the Alberta Geological Survey*, 41, 151p.
- Smarrt, P.F.M., and Granger, J.E.A., 1974, Sampling for vegetation survey: some aspects of the behavior of unrestricted, restricted, and stratified techniques, *Journal of Biogeography*, 1, 193-206.
- Sneed, E.D., and Folk, R.L., 1958, Pebbles in the lower Colorado River, Texas, a study in particle morphogenesis, *The Journal of Geology*, 66, 114-150.
- Thorson, R.M., 1989, Glacio-isostatic response of the Puget Sound area, Washington, *Geological Society of America Bulletin*, 101, 1163-1174.
- U.S. Geological Survey, 1945, Surface water supply of the United States, 1943, Part 12, Pacific Slope Basins in Washington and Upper Columbia River Basin: U.S. Geological Survey Water Supply Paper 982, 257 p.
- U.S. Geological Survey, 1946, Surface water supply of the United States, 1944, Part 12, Pacific Slope Basins in Washington and Upper Columbia River Basin: U.S. Geological Survey Water Supply Paper 1012, 261 p.

- U.S. Geological Survey, 1947, Surface water supply of the United States, 1945, Part 12, Pacific Slope Basins in Washington and Upper Columbia River Basin: U.S. Geological Survey Water Supply Paper 1042.
- U.S. Geological Survey, 1948, Surface water supply of the United States, 1946, Part 12, Pacific Slope Basins in Washington and Upper Columbia River Basin: U.S. Geological Survey Water Supply Paper 1062.
- U.S. Geological Survey, 1949, Surface water supply of the United States, 1947, Part 12, Pacific Slope Basins in Washington and Upper Columbia River Basin: U.S. Geological Survey Water Supply Paper 1092.
- U.S. Geological Survey, 1950, Surface water supply of the United States, 1948, Part 12, Pacific Slope Basins in Washington and Upper Columbia River Basin: U.S. Geological Survey Water Supply Paper 1122.
- Werrity, A., 1992, Downstream fining in a gravel-bed river in southern Poland: lithologic controls and the role of abrasion, *in* Dynamics of Gravel Bed Rivers, P. Billi, R.D. Hey, C.R. Thorne and P. Tacconi, eds., J. Wiley and Son, Chichester, p. 333-350.
- Wolman, M.G., 1954, A method of sampling coarse river-bed material, Transactions American Geophysical Union, 35, 951-956.



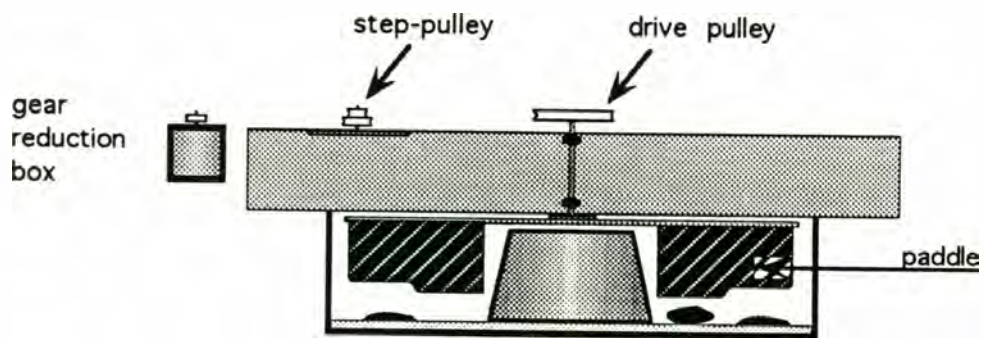
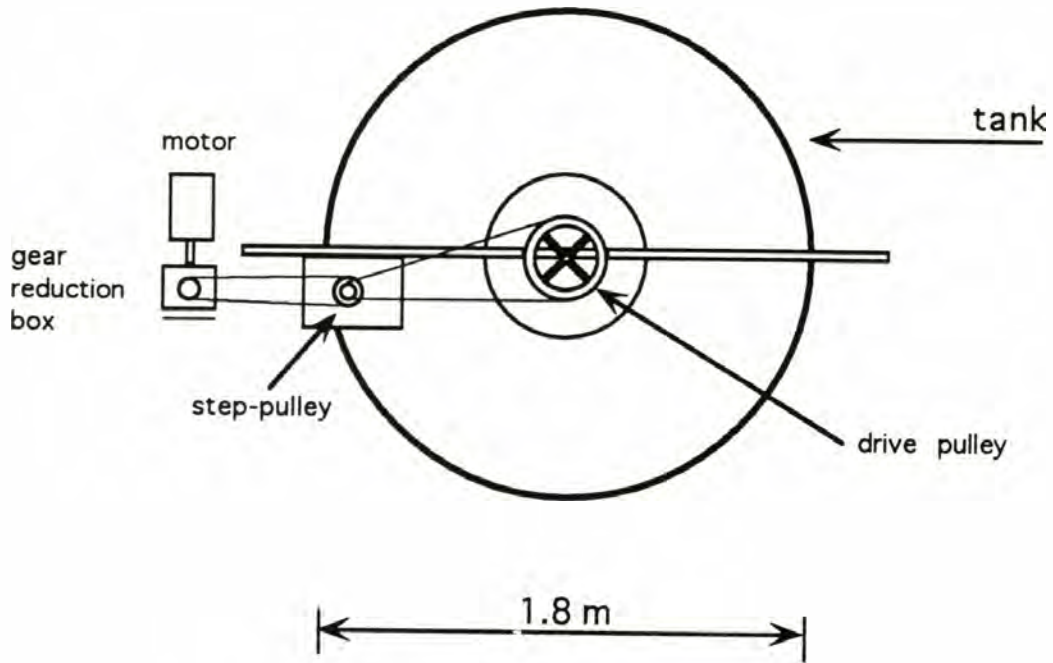
## APPENDIX

The abrasion tank (Figure 14) was modeled after that used by Kuenen (1956, Figure 2). The apparatus was constructed using a 1.8 m (six-foot) diameter metal tank that was 0.45 m (1.5 feet) deep. Small cobbles were embedded in concrete on the floor. In the center was a metal pillar, which provided a tapered-walled circular channel 0.4 m (1.3 feet) deep, 0.61 m (2.0 feet) wide, and about 5.49 m (18 feet) around the outside diameter. Two paddles were constructed of PVC and were driven by a one-horse power motor, stepped down through a gear reduction box and a series of step-pulleys. The paddles propelled water around the channel and this current moved the particles. All particles, from the largest cobbles to sand, had a tendency to collect in the low-velocity zone on the inside of the channel. This problem was corrected by increasing the taper on the inside wall, and by cutting the paddles short on the outside and long on the inside.

Each pair of particles were transported for the calculated amount of time it would take to transport the slowest particle a distance of 2500 m. In all cases the foliated particle was the slowest particle in a pair. The time was calculated by

$$T = (2500 \text{ m}) \times (1 \text{ minute} / N) \times (1 \text{ revolution} / 5.5 \text{ m})$$
where T is the total required time in minutes and N is the number of revolutions made by the slowest particle in one minute.

Plan view



Cut-away view

Figure 14. Schematic drawing of the abrasion tank.